PTP74-17622

IMMEDIATE SOLAR-ENERGY UTILIZATION USING GREENHOUSE BULK CURING AND DRYING SYSTEM

B. K. HUANG and C. G. BOWERS, JR.
Department of Biological and Agricultural Engineering
North Carolina State University
Raleigh, North Carolina 27607

July 1976

FINAL REPORT FOR THE
PERIOD JANUARY 1975 — APRIL 1976

Prepared for
ENERGY RESEARCH AND DEVELOPMENT ADMINISTRATION
NATIONAL SCIENCE FOUNDATION
Washington, D.C.

IMMEDIATE SOLAR-ENERGY UTILIZATION

USING GREENHOUSE BULK CURING AND DRYING SYSTEM

July 1976

Research Performed Under Grant No. PTP74-17622

B.K. Huang, Professor
C.G. Bowers, Jr., Research Assistant

North Carolina State University
Biological and Agricultural Engineering Department
Raleigh, North Carolina 27607

PREFACE

This research program "Immediate Solar-Energy Utilization Using Greenhouse Bulk Curing and Drying System" was conducted at the North Carolina State University, Biological and Agricultural Engineering Department, Raleigh, N.C. 27607. It was initiated under the National Science Foundation, Grant Number PTP74-17622, and then transferred to the Energy Research and Development Administration.

The authors wish to acknowledge the partial sponsorship for the research by the National Science Foundation, the Energy Research and Development Administration, the U.S. Department of Agriculture, and the North Carolina Agricultural Experiment Station. They wish to express their appreciation to: Dr. D.H. Willits, Assistant Professor of Biological and Agricultural Engineering and Dr. P.V. Nelson of Horticultural Science for conducting studies on energy savings and flower production during greenhouse operation; Mr. H.S. Chang, Associate Professor of Agricultural Engineering, National Taiwan University for performing circuit simulation analysis and verification; Mr. W.R. Baker, Superintendent, and Mr. A.T. Wood, Tobacco Supervisor, of Central Crops Research Station for participating in field tests; Dr. F.J. Hassler, Head and Professor, Dr. W.H. Johnson, Professor, Dr. C.F. Abrams, Assistant Professor, and Mr. R.W. Watkins, Associate Professor of Biological and Agricultural Engineering, and Mr. D.W. Barnes, Jr., Assistant Professor of Architecture for consultation, and Mrs. Brenda Mason, Secretary of Biological and Agricultural Engineering for her typing of the manuscript, and Dr. K.R. Keller, Director of Agricultural Experiment Station for his encouragement and continuous support for this research.

The use of trade names in this publication does not imply endorsement by the North Carolina Agricultural Experiment Station of the products named, nor criticism of similar ones not mentioned.

ABSTRACT

Solar energy utilization in a greenhouse bulk curing system was investigated. The system used two basic approaches to the capture and storage of solar energy. First, as a bulk curing structure incorporating dehydration and electric power saving features, it was designed to directly collect, store and use energy from the sun to cure tobacco. Second, as a greenhouse solar energy was used for photosynthesis for maximum plant growth under a controlled environment. The collection, consumption, and storage of solar energy in this system was studied using air as the heat transfer medium.

Two greenhouse bulk curing and drying systems were designed, constructed and field tested under this project. The basic parts of the systems are: bulk curing module with solar heat absorbers, portable frames to support tobacco, and a heating unit with temperature and air flow controls; and a specially designed greenhouse with curing and heating unit rooms, gravel energy storage channels, air flow controls, and an auxiliary fan for efficient movement of air over the solar absorbers and through the gravel. During greenhouse operation, the solar absorbers and portable frames are removed, and the facility is used to grow flowers and tobacco transplants.

Using solar energy as a first source of energy in tobacco curing, a 37 percent fuel savings was achieved as compared to a conventional bulk curing barn. Solar energy was effectively used to heat air for immediate use in curing and/or for storing energy in gravel for nighttime use. With the electricity costs for operation of the conventional main furnace fan being almost as much as the fuel costs for curing, the auxiliary fan should substitute for the main fan during latter stage of drying. Then, only about one-fourth the power of the main fan would be required.

Thermal circuit simulation was used to analyze solar energy collection and air preheating for tobacco curing in the greenhouse bulk curing and drying system. Initial results of the simulation for predicting the actual temperatures of the solar preheated air agreed quite well with experimental results. Improvements in the thermal circuit model are being made to more accurately predict collector air temperatures during curing. The gravel energy storage system is also to be added to the model.

The greenhouse bulk curing and drying system provides an efficient means of utilizing solar energy in tobacco curing and greenhouse crop production. In this multipurpose farm structure, attention to costs of construction and materials resulted in the greenhouse bulk curing system costing slightly less than that of conventional bulk barn of equivalent capacity.

TABLE OF CONTENTS

LIST OF FIGURES

LIST OF FIGURES (CONTINUED)

LIST OF TABLES

INTRODUCTION

The energy situtation has forced an awareness upon the agricultural and industrial community that energy is a valuable resource which must be efficiently and conservatively used. Research efforts in agriculture until now have concentrated on developing technology to increase yields and mechanize crop production. Energy requirements to accomplish these advancements were not a major concern. The current costs and actual availability of energy to support agricultural production are realigning research priorities. Alternative energy sources and more efficient energy processes must be utilized.

Solar energy is a readily available, alternative energy source which can be used in the curing and drying of farm crops. The daily and seasonal energy variation, along with the collection and utilization equipment costs for solar energy have, in the past, slowed development of this alternative energy source. Today's energy situation provides a unique opportunity for the utilization of solar energy as a supplemental energy source for certain farm operations.

Current curing and drying of tobacco utilizes the bulk curing process (3,10) which involves the passage of conditioned air through tightly packed tobacco. As compared to non-bulk curing, bulk curing improves the control of the process variables of temperature, humidity, and air flow, and reduces the labor and fuel requirements. With tobacco curing being done in the summer months of July and August when the sun's energy is most readily available, the bulk curing process should utilize solar energy to save fuel for economical farm operation.

The greenhouse bulk curing system, developed by Huang et al (2,4,5) consists of a bulk curing module inside a specially designed greenhouse. It uses two basic approaches to the capture and storage of solar energy. First, as a bulk curing structure, it was designed to utilize physical equipment to directly collect, store and use energy from the sun to cure tobacco. Second, as a greenhouse in which the solar absorbers and some curing equipment are removed, solar energy is used for growing horticultural/floricultural plants and tobacco transplants. This multipurpose farm structure provides an efficient means of utilizing solar energy in tobacco and greenhouse crop production.

The overall objective of this project was to investigate the utilization of solar energy in tobacco bulk curing and greenhouse crop production using a greenhouse bulk curing system. The research involved the design and construction of the greenhouse bulk curing system, experimental testing of the system to fully evaluate solar energy utilization, determination and optimization of system design parameters, data analysis, system modeling, and computer simulation with verification using the acquired data. The main emphasis of the project was to evaluate the solar energy utilization of the system in tobacco curing. However, the structure was also evaluated for greenhouse crop production and tobacco seedling growth.

DESIGN AND CONSTRUCTION OF GREENHOUSE BULK CURING AND DRYING SYSTEM

The greenhouse bulk curing and drying system relates to a farm structure that may be utilized as either a curing and drying facility or as a plant growth facility. The system allows maximum utilization of available solar energy for fuel savings and plant production. As a greenhouse type of structure, it is an inherent, efficient solar energy collector. With the addition of solar absorbers and curing equipment for use in the bulk curing mode, solar energy is used to cure and dry the tobacco. In the greenhouse mode, solar energy is effectively used to photosynthesize plants under a controlled environment for maximum food or plant production.

The structure basically consists of: (1) a flat concrete slab and block wall foundation, (2) a transparent exterior with clear corrugated fiberglass, (3) frames to support tobacco racks or seedling growing and handling trays, (4) a heating unit with temperature, humidity, and air flow controls, and (5) air vents and ducts for air flow control. Two types of structures can be designed for the greenhouse bulk curing and drying system - load-supporting wall design or shell design.

Structure Orientation

The orientation of the structure for maximum solar energy collection was evaluated by computer simulation of the incident solar radiation and the structure shape for a one foot wide section using a program developed by Mr. D.W. Barnes*. A north-south orientation of the axis of a semicylindrical greenhouse receives the highest annual solar radiation and also receives the highest monthly solar radiation for the months of June, July, and August. These months are of prime importance for tobacco curing.

*Personal communication between D.W. Barnes and C.G. Bowers, Jr., 1975.

The structure for the greenhouse bulk curing and drying system was oriented north-south. The south end was used as the loading and entrance end so as to add to the amount of incident solar energy available for collection and utilization. Exposed walls on the north end but facing south were painted black.

Load-Supporting Wall Design

The general design of the greenhouse bulk curing system using the load-supporting wall design is shown in perspective view in Figure 1. The side elevation-sectional view of the structure illustrating its use as a tobacco curing and drying facility is shown in Figure 2. Corrugated fiberglass is used for the exterior and is preferable to flat fiberglass. For a given area of structure corrugated fiberglass provides a greater surface area so that more solar radiation can be intercepted. It also provides more rigidity in the structure. The transmitted solar radiation is captured or absorbed by the heat absorber, which is preferably of a near-thermally black material positioned immediately inside of the structure sides and top. The heat is transferred to the material to be cured and dried by forced air moving continuously inside the system. The heat absorber as shown in Figures 2 and 3 acts to confine the system of forced air to the area occupied by the bulk tobacco. This configuration assures uniform distribution of heat and air through the tobacco. The heat absorber also functions to shield the tobacco from excessive exposure to the sunlight to prevent undesirable product discoloration. The dead air spaces between the transparent exterior and the heat absorber serve as an insulation against conduction losses. The temperature sensor in the duct controls proper air-flow and furnace heating as needed to insure proper curing conditions. The slab and block foundation support the upper structure and serve as partial heat storage for excess solar energy.

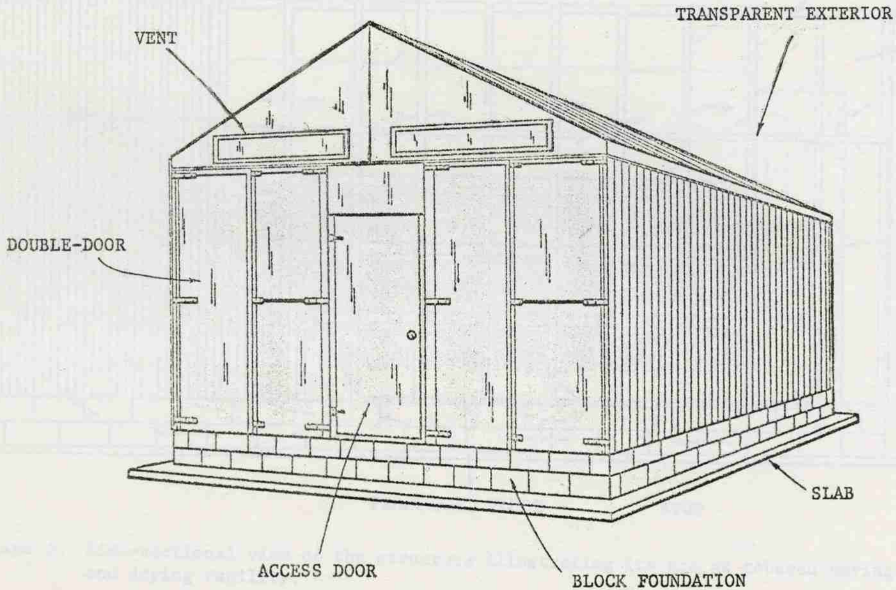

Figure 1. Perspective view of greenhouse bulk curing and drying system with load-supporting wall design.

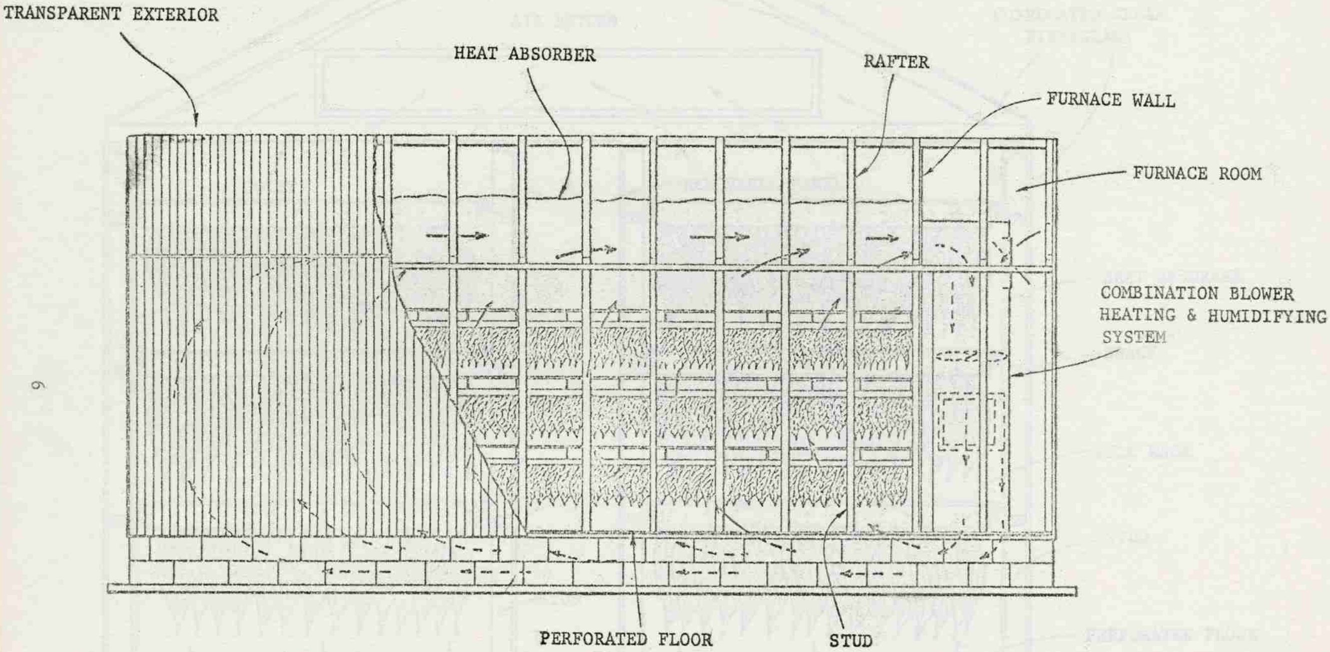

Figure 2. Side-sectional view of the structure illustrating its use as tobacco curing and drying facility.

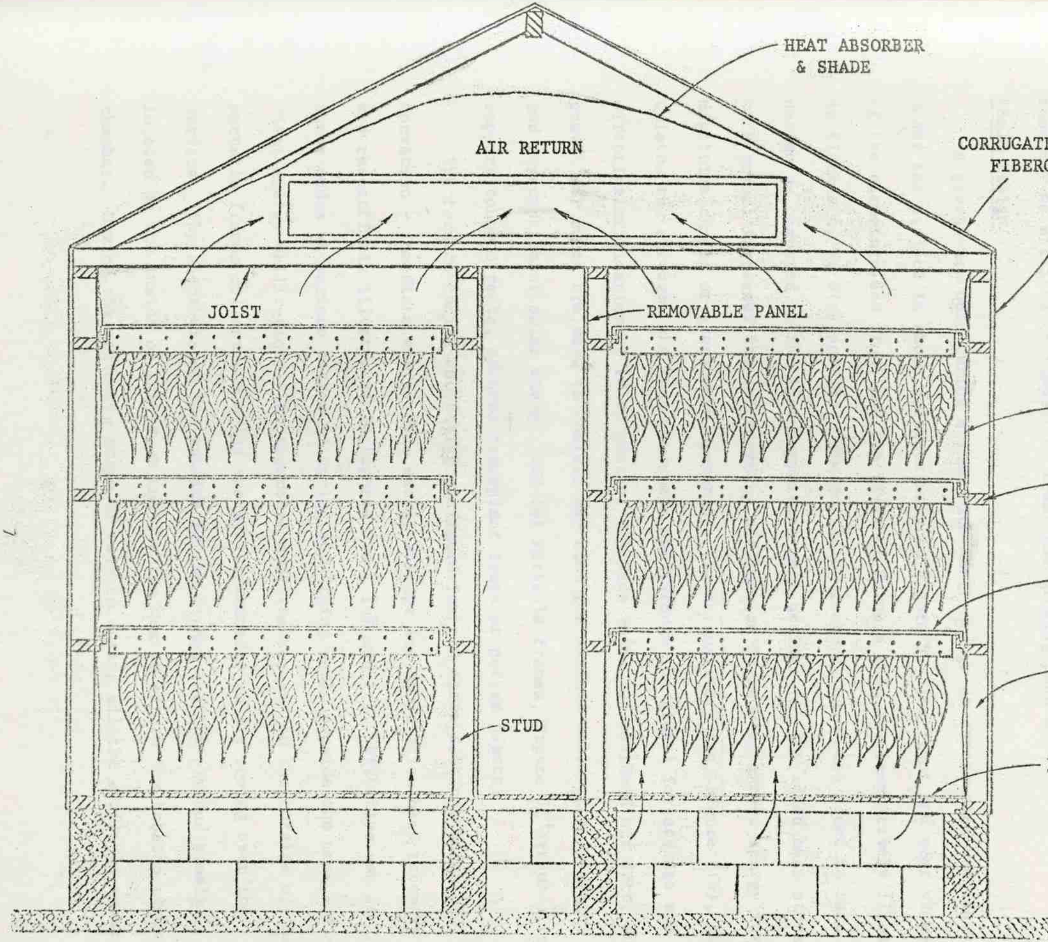

Figure 3. Cross-sectional view of the structure with load-supporting wall design illustrating its use as tobacco curing and drying facility.

The cross-sectional views of the structure with load-supporting wall design, Figures 3 and 4, show respectively the system being used as a tobacco curing facility and plant growing facility. The enclosing structure wall is designed to support the loaded bulk racks or the plant growing trays. The middle access room may be utilized to inspect or treat the growing plants.

Shell Design

A greenhouse bulk curing system with shell design as constructed and tested under the project is shown perspectively in Figure 5. The front and rear views of the structure, and front and top views of furnace room are respectively illustrated in Figures 6, 7, 8(a) and (b). The following features have been added to this design as compared to the load-supporting wall design: (1) The added heat storage with gravel increases the solar energy utilization by storing excess energy for nighttime curing or greenhouse operation, (2) An auxiliary fan, Figure 8(b), circulates the air over the heat absorbers and through the gravel for storage and effective utilization of solar energy, (3) Side vents, an overhead air duct, and gravel air ducts are used to control air flow for maximum collection, storage, and consumption of solar energy, and (4) Portable frames, Figure 5, are used to support tobacco racks, tobacco transplant trays or potted plants.

The tobacco curing and drying configuration and three distinct modes of operation - immediate energy use, energy storage and dehydration heat recovery are respectively illustrated in Figures 9(a), (b) and (c). Effective use of these modes at various stages of curing and drying would provide the most efficient energy utilization. The absorbers over the top and on the outside of the portable frames collect the solar energy for transfer to air moving over the surface. The absorbers on the outside of the frames and the plywood panels located on the inside of the frame confine the heated air to the tobacco curing chamber. During the yellowing stage of tobacco curing all the available solar

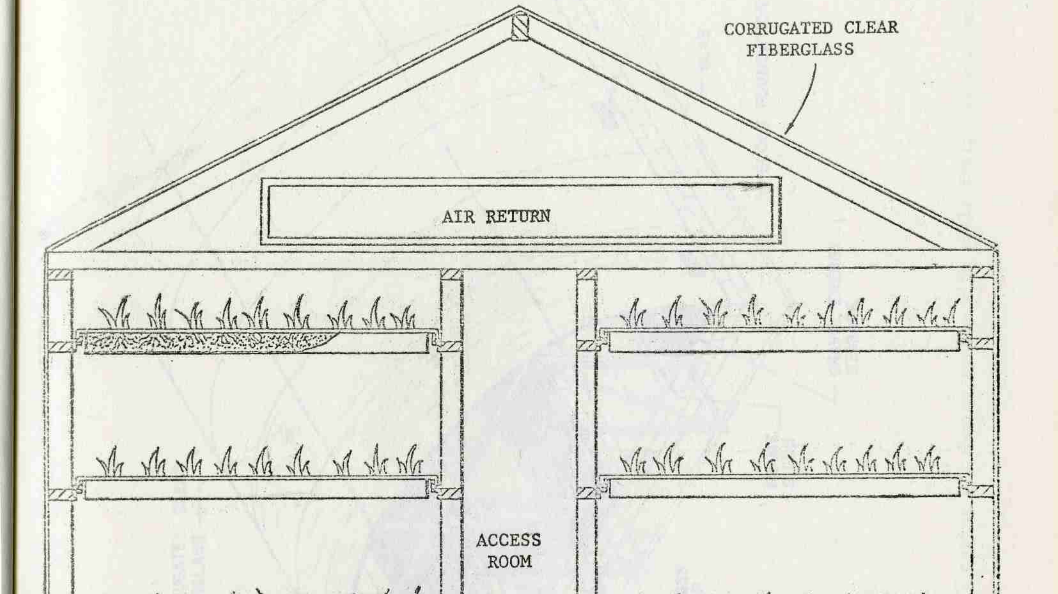

Figure 4. Cross-sectional view of the structure with load-supporting wall design illustrating its use as plant growing facility.

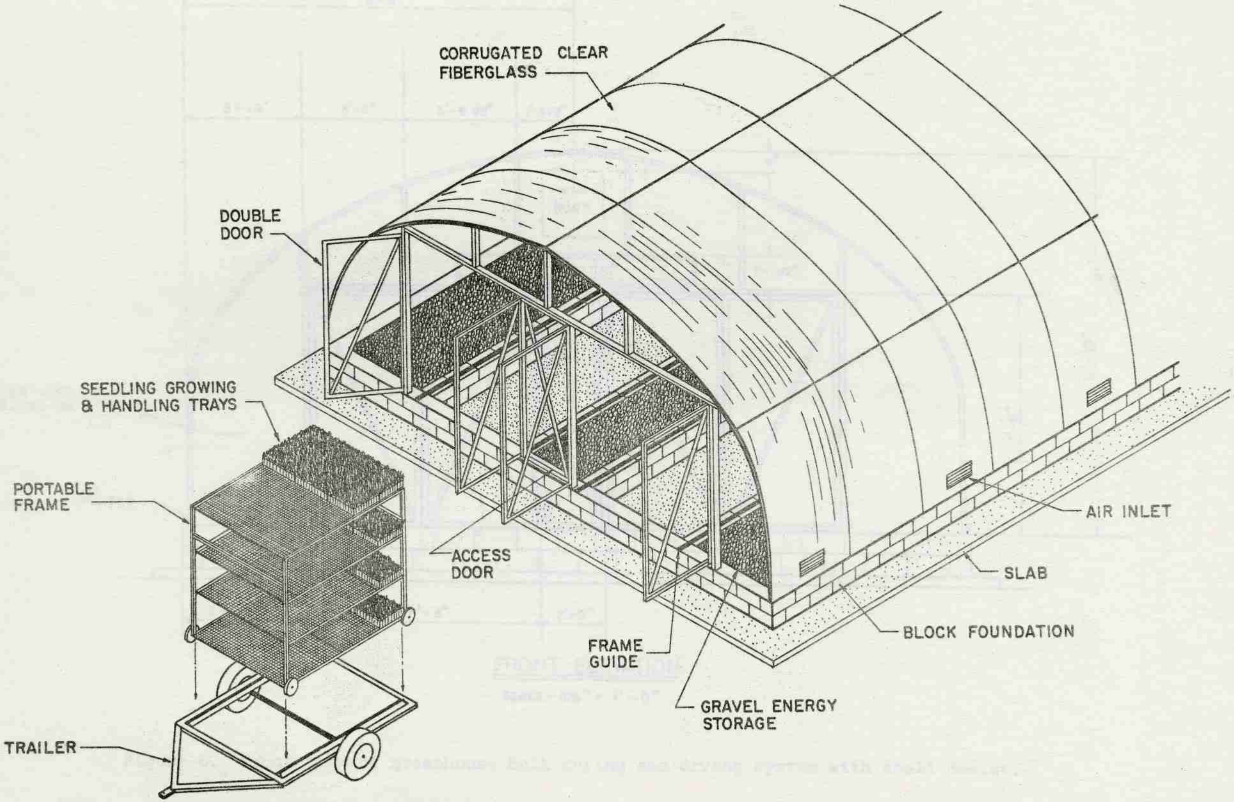

Figure 5. Perspective view of greenhouse bulk curing and drying system with shell design showing mobile handling system

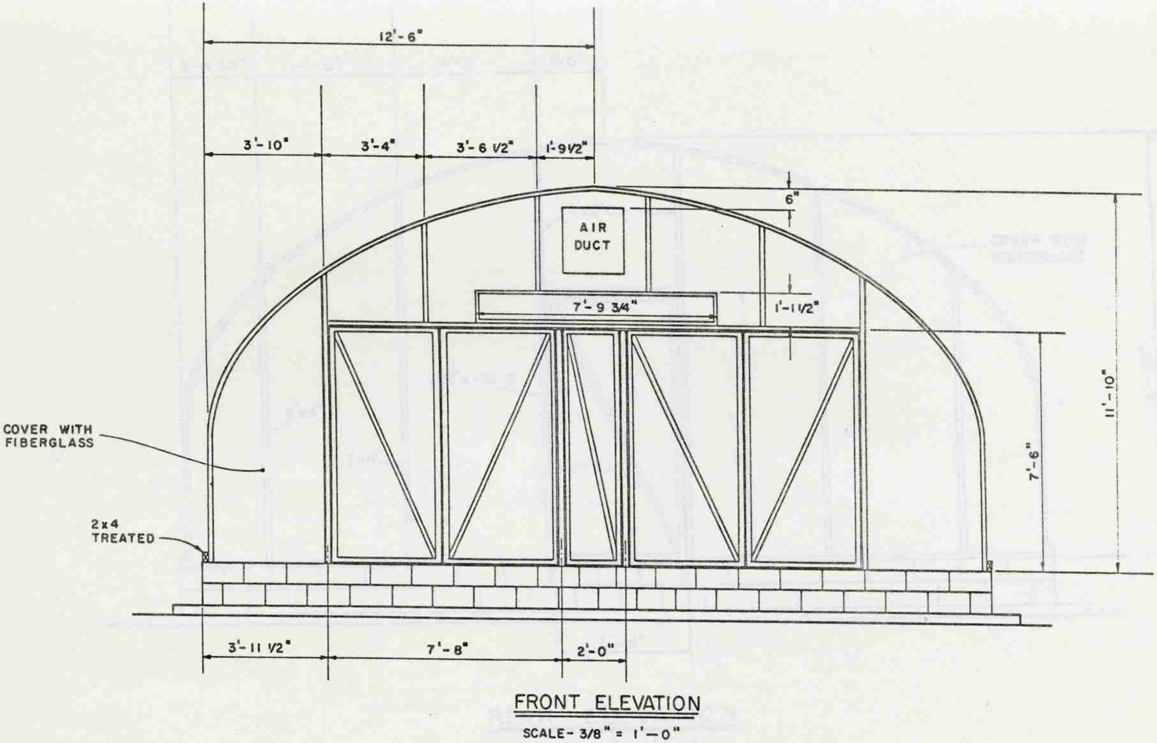

Figure 6. Front view of greenhouse bulk curing and drying system with shell design.

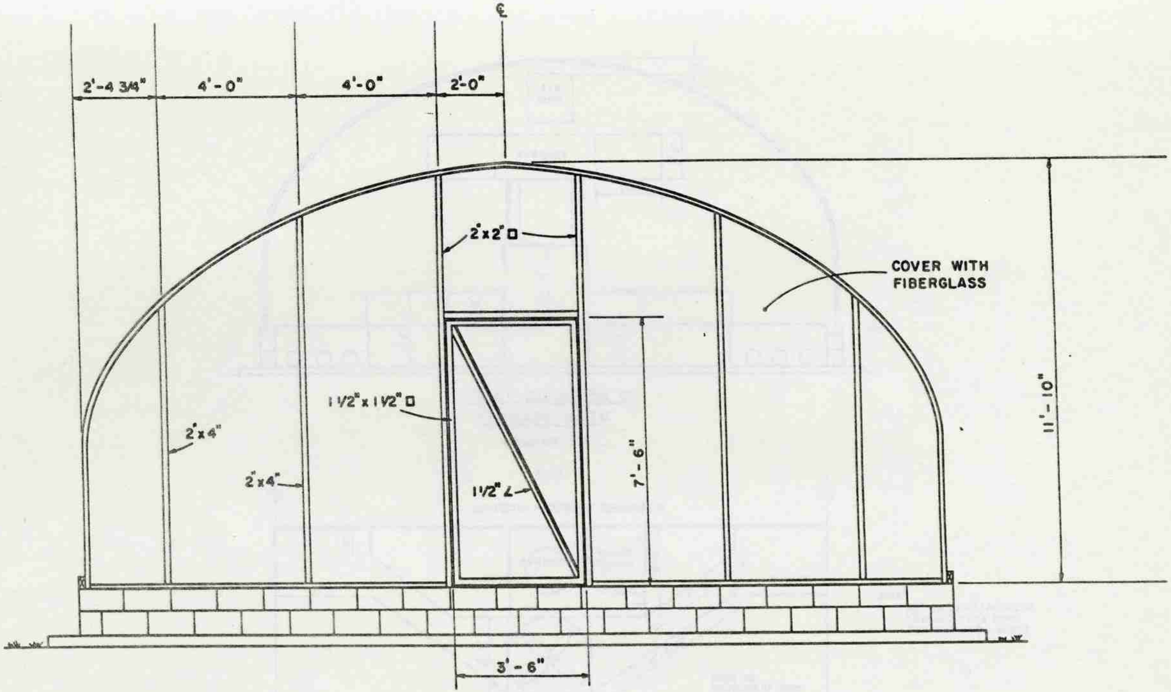

REAR ELEVATION

SCALE - 3/8" = 1'-0"

Figure 7. Rear view of greenhouse bulk curing and drying system with shell design.

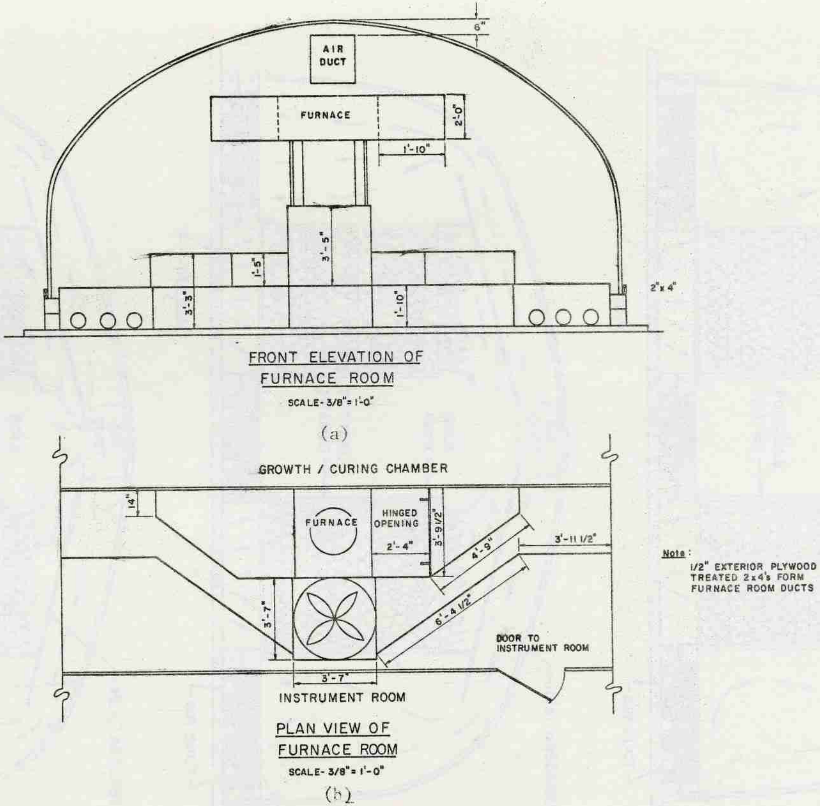

Figure 8. Furnace room for greenhouse bulk curing and drying system with shell design: (a) Front view and (b) Top view.

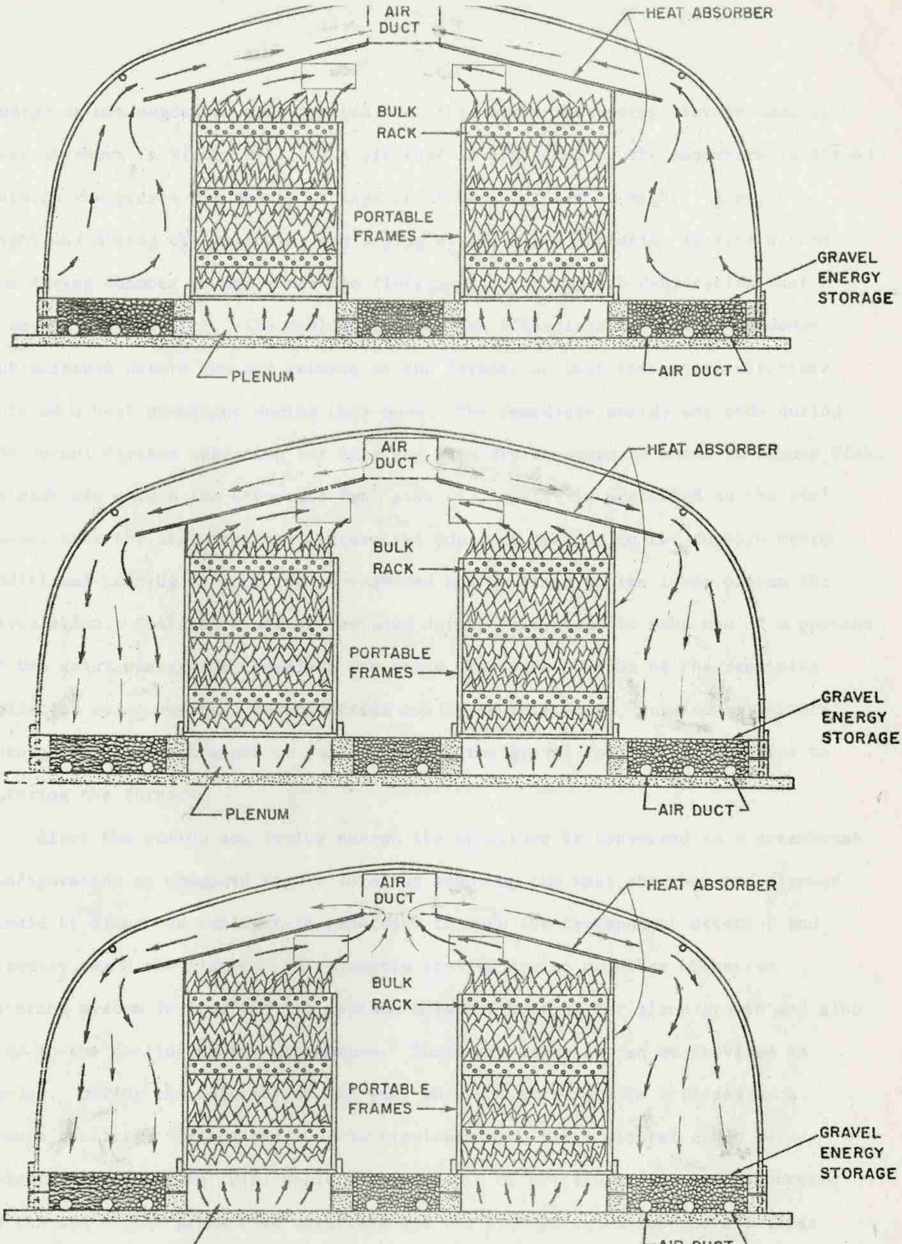

Figure 9. Cross-sectional view of greenhouse bulk curing and drying system with shell design being used to cure tobacco: (a) Immediate daytime energy use, (b) Daytime energy storage for night use and (c) Dehydration heat recovery during nighttime yellowing.

energy is not needed to cure tobacco. At this stage the energy storage mode is used as shown in Figure 9(b). The air that is preheated by the absorbers is forced through the gravel for energy storage and subsequent use at night. Also, at night and during the yellowing and drying stage, air circulation is from within the curing chamber to-and-under the fiberglass to accomplish dehydration-heat recovery, Figure 9(c). The cool surface of the fiberglass is used to condense out moisture before the air returns to the furnace so that the entire structure acts as a heat exchanger during this mode. The immediate energy use mode during the normal daytime operation for leaf and stem drying stage is shown in Figure 9(a). Outside air enters the structure from side air inlets, is preheated as the air passes over the heat absorber, enters the top duct leading to the furnace where additional heating is supplied as required and is blown to the lower plenum for circulation. Combined modes can be used during this stage to make use of a portion of the solar energy for immediate use while storing a portion of the remaining collected solar energy. For nighttime curing in this stage, outside air enters through the side vents and is pulled through the gravel for preheating prior to entering the furnace.

After the curing and drying season the structure is converted to a greenhouse configuration as shown in Figure 10(a) by removing the heat absorber and plywood panels to allow the sunlight to penetrate through the transparent exterior and directly reach the plants. An automatic misting device or other effective watering system is provided for optimum moisture control for plant growth and also aids in the cooling of the greenhouse. Auxiliary lighting can be provided as needed. During the majority of the year when the structure is utilized as a growth facility, various types of horticultural and floricultural crops as illustrated in Figure 10(b) would be produced. Of particular interest, however, is the use of the greenhouse structure for the production of tobacco seedlings

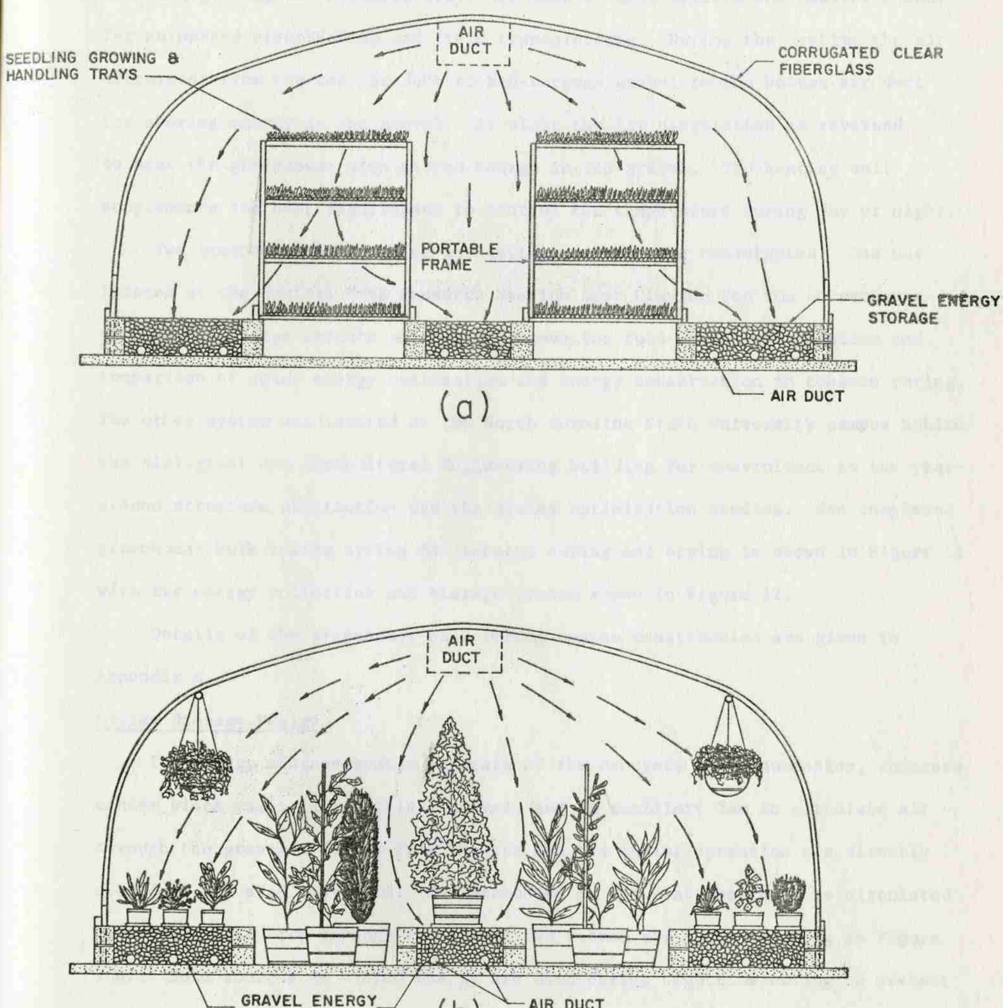

Figure 10. Cross-sectional view of greenhouse bulk curing and drying system with shell design being used as greenhouse: (a) Tobacco transplant production and (b) Horticultural crop production.

under a fully controlled environment using the arrangement shown in Figure 10(a). Seedling growing and handling trays are used to grow uniform and healthy plants for automated plantbedding and field transplanting. During the daytime the air circulates from the top air duct to-and-through gravel to the bottom air duct for storing energy in the gravel. At night the air circulation is reversed to heat the greenhouse with stored energy in the gravel. The heating unit supplements the heat requirement to control the temperature during day or night.

Two greenhouse bulk curing and drying systems were constructed. One was located at the Central Crop Research Station near Clayton for the convenience of obtaining large amounts of tobacco leaves for full scale investigation and comparison of solar energy utilization and energy conservation in tobacco curing. The other system was located at the North Carolina State University campus behind the Biological and Agricultural Engineering building for convenience in the year-around structure utilization and the system optimization studies. The completed greenhouse bulk curing system for tobacco curing and drying is shown in Figure 11 with its energy collection and storage system shown in Figure 12.

Details of the greenhouse bulk curing system construction are given in Appendix A.

System Storage Design

The energy storage system consists of the concrete slab foundation, concrete cinder block walls, air ducting, gravel, and an auxiliary fan to circulate air through the gravel. Energy from the sun and the curing operation are directly stored in the slab and walls. Air preheated by the heat absorbers is circulated by the auxiliary fan through the gravel and bottom air ducts as shown in Figure 9(b). Both sources of stored energy are used during nighttime curing to preheat the air prior to entering the furnace.

Figure 11. Greenhouse bulk curing and drying system during tobacco curing and drying operation.

Figure 12. Energy collection system showing side and top absorbers, fiberglass exterior and frame, and gravel energy storage.

Slotted, corrugated plastic pipe was used for the air passage ducts under the gravel. This corrugated pipe provided the following advantages: (1) The pressure drop caused by the friction loss produced by the corrugations almost exactly offset the static pressure gain through the pipe. This result produces a uniform air flow through the slotted pipe openings and into the gravel, (2) The strength of the corrugated pipe easily supports the gravel on top of it, and (3) It is readily available as regular soil-water drainage pipe.

Experimental tests were conducted to measure air flow and pressure losses through the corrugated drainage pipe. The slot size and spacings were determined so as to give the most uniform air flow through the gravel. A computer program was developed to evaluate various parameters such as air flow, resistance, opening, etc. The results of the computer program closely conformed to the test data.

The auxiliary fan was selected so as to produce between 4000 and 5000 cfm at 1/2 inch static pressure. This air flow is approximately the total fresh air intake needed during maximum curing and drying of the tobacco contained in the designed structure.

Gravel for storing the solar energy should be in the size range from 1/2 to 2 inches. Actual gravel used in the test during the summer, 1975 were crushed granite varying in size from 1/4 inch to 1 1/2 inches.

SYSTEM TESTING AND INSTRUMENTATION

The greenhouse bulk curing and drying system was tested for tobacco curing, flower production, and tobacco seedling production. The tobacco curing was done during August and September, 1975. Klanchoe flowers were grown from November 1975 through February 1976 with the structure in the greenhouse mode. Tobacco seedlings were grown in March and April of 1976.

Testing Procedure for Curing and Drying

The greenhouse bulk curing structure was first set for the drying mode. Figure 13 shows the curing and drying chamber formed by the top air duct, heat absorbers and portable frame. Field loading of tobacco using the bulk racks is shown in Figure 14.

The following procedure was generally used during curing and drying of tobacco:

(1) The bulk racks were filled and placed on the portable frames. The curing section of the structure was sealed when completely filled with tobacco.

(2) The furnace was fired, and a "normal" bulk curing schedule followed. The temperature curing scheduled generally consisted of two-three days yellowing at 90^{o}-95^{o}F, three days of leaf drying in which the temperature was advanced from 90^{o}F to 170^{o}F at 2^{o} to 3^{o}F per hour, and one day of stem drying at 170^{o}F. During leaf drying the temperature was held at certain levels as determined by tobacco conditions. The actual schedule followed for each cure was modified slightly to accommodate varying tobacco conditions and curing characteristics.

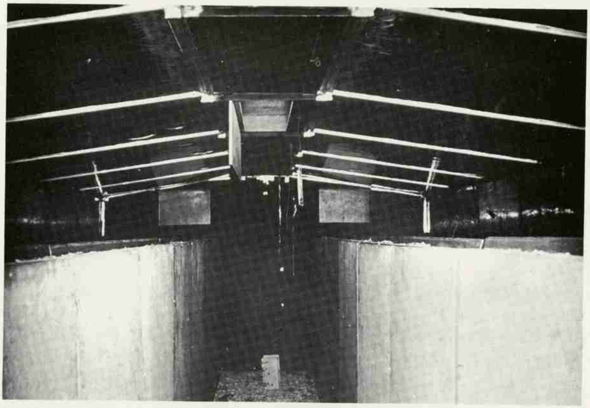

Figure 13. Inside view of greenhouse bulk curing system showing top air duct, absorber/insulators, and portable frames.

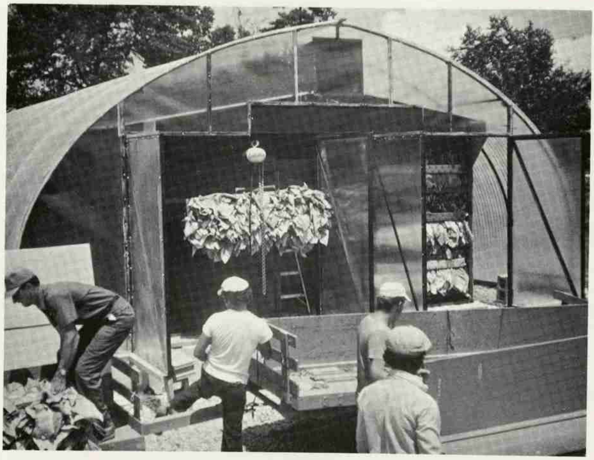

Figure 14. Field loading of tobacco in greenhouse bulk curing barn using bulk tobacco racks.

(3) During the cure the fresh air intake of the furnace was set as needed by the degree of drying required for each stage of curing. Generally the intake was closed during yellowing, gradually opened during initial leaf drying until about 50% fresh air was being used at approximately $125^{\circ}$to 135°F, then gradually reduced during the latter stages of leaf drying until it was completely closed at 170°F. The intake was kept closed during stem drying at 170°F.

(4) Air preheated by either the absorber or the gravel was used as input to the furnace both during day and night operation as shown by Figure 9 and as discussed in the previous section.

Instrumentation

Instrumentation for monitoring the test conditions and variables consisted of a digital data acquisition system with thermocouples to measure temperature, a strip chart recorder for monitoring radiation levels measured by a pyranometer, and an LP gas meter to measure fuel consumption. Wind speed and direction detectors for outside conditions are to be added as inputs to the systems. Air flow sensors for measuring air flow inside the structure are to be added also.

The digital monitoring system recorded up to 50 individual data points using thermocouple transducers, an ice point reference, a scanner, a millivoltmeter with BCD output, a digital clock, teletype interface, and teletype. The interface converts the BCD output of the millivoltmeter to a digital code compatible with the teletype. The clock initiates the scanner to read thermocouple voltages at prescribed intervals.

Copper constant thermocouples were used to measure ambient air temperatures, collector-air and-surface temperatures, gravel temperatures, and curing air and tobacco temperatures. For air temperatures shielded thermocouples were used to measure both dry and wet bulb temperatures. Surface temperature measurements were made by attaching the thermocouples to the surface of the material. Thermocouples were placed within the tobacco racks to measure the tobacco bulk temperature. All temperature measurements were taken at 30 minute intervals.

Total horizontal radiation was sampled at two second intervals using a multipoint recorder and a pyranometer. The LP gas meter was manually read at approximately 30 minute intervals during the day and two or three times at night.

The same instrumentation was used to measure temperature distribution, radiation, fuel consumption, and air flow during the greenhouse operation for growing Klanchoes and tobacco seedlings. Exhaust vent fans, an auxiliary heater, and temperature controls were added for the greenhouse operation. Greenhouse temperatures were maintained during both Klanchoe and tobacco seedling production as follows: (1) For temperatures above $85^{o}F$, the exhaust fans were used to exchange inside air and fresh air, (2) Between 80^{o} and $85^{o}F$, the auxiliary fan circulated air within the greenhouse to heat the gravel and cool the air, (3) During the daytime for temperature from 70^{o} to $80^{o}F$, no air movement occurred, (4) At nighttime, no heating occurred until the temperature dropped below $63^{o}F$ at which time the auxiliary fan came on to heat the greenhouse with energy stored in the gravel; the auxiliary heater turned on below $60^{o}F$. The potted Klanchoes were placed in the greenhouse in November, 1975 and removed in March, 1976 just after they had flowered. The tobacco seedling growing and handling trays were placed in the greenhouse in April, 1976 and removed in May, 1976.

CURING AND DRYING OPERATION OF GREENHOUSE BULK CURING AND DRYING SYSTEM

During the summer of 1975, four full barns of tobacco were cured in the greenhouse bulk curing structure. These curing tests were conducted from August 6 through September 12, 1975. Fuel consumption, temperature, and radiation data were automatically recorded during curing operations. Qualitative observations were made to assure good quality curing during the tests. As experience with the system was gained and as data were analyzed, operational control changes were determined based on weather and tobacco curing conditions. Results are presented here for discussion.

Maximum solar radiation levels during a typical curing day for direct plus diffuse radiation varied from 250 to 300 BTU/ft^2 hr. Typical surface temperatures of the heat absorbers during the day for almost no air movement are shown in Figure 15. Absorber temperatures were a maximum when the sun was perpendicular to the surfaces. The variations at 12:30 PM and 3:00 PM were caused by a change in the ventilation configuration of the structure during the yellowing phase of the cure. The tobacco temperature was higher than needed for acceptable yellowing of the tobacco. The entire structure was vented from 12:30 PM to 3 PM to reduce heat buildup. The vents were returned to the normal daytime yellowing configuration at 3 PM.

During yellowing when fresh air intake for drying was minimal, the solar energy collected by the greenhouse bulk curing system during the clear sky, peak solar radiation was more than could be immediately transferred to the gravel for energy storage. The bulk tobacco temperatures increased above $100^{\circ}F$. The structure had to be vented to decrease the system's overall temperature.

A comparison between the outside air temperature and air temperature over the heat absorbers for an entire cure is shown in Figure 16. The inside temperature

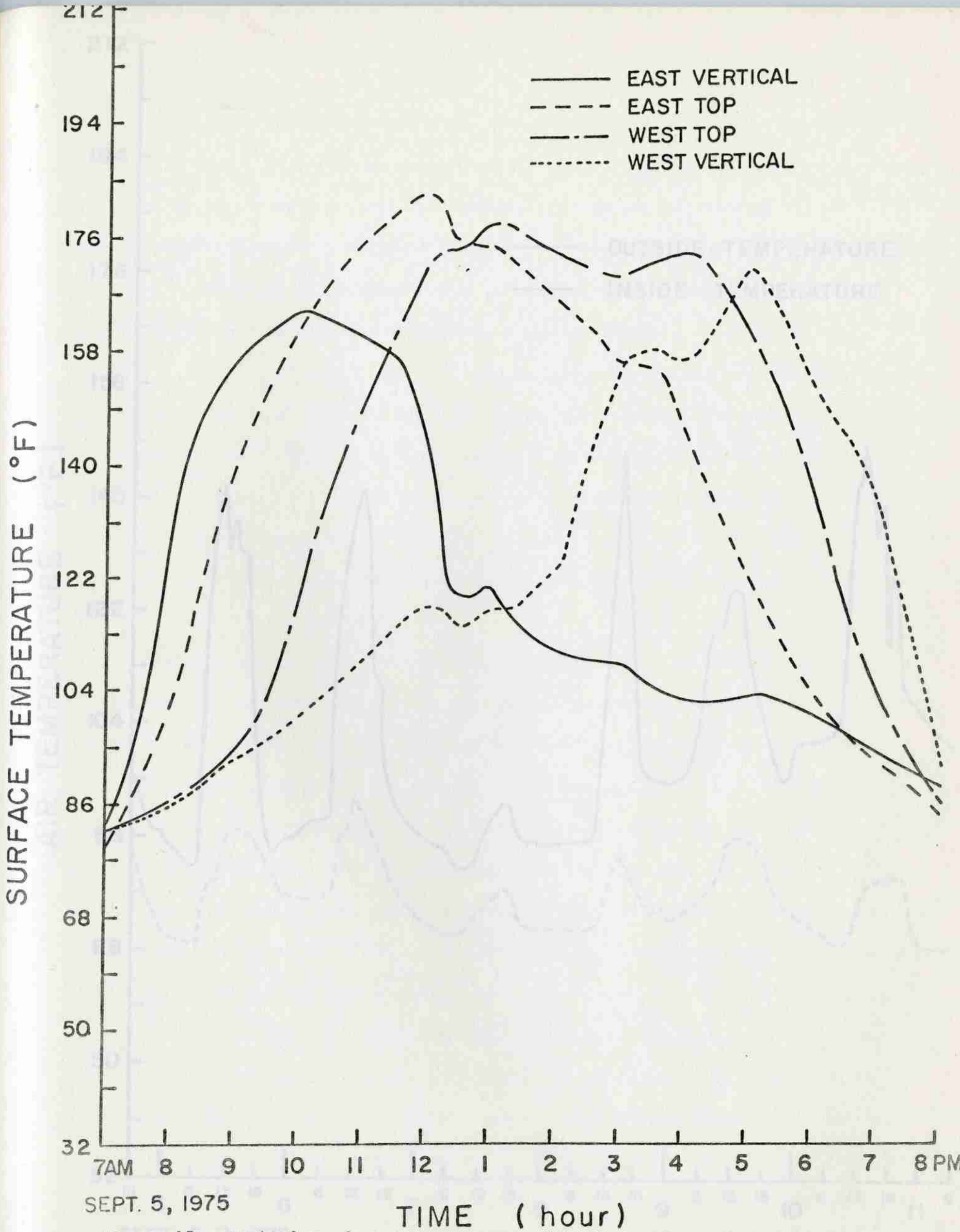

Figure 15. Typical surface temperatures of heat absorbers during early stages of bulk curing.

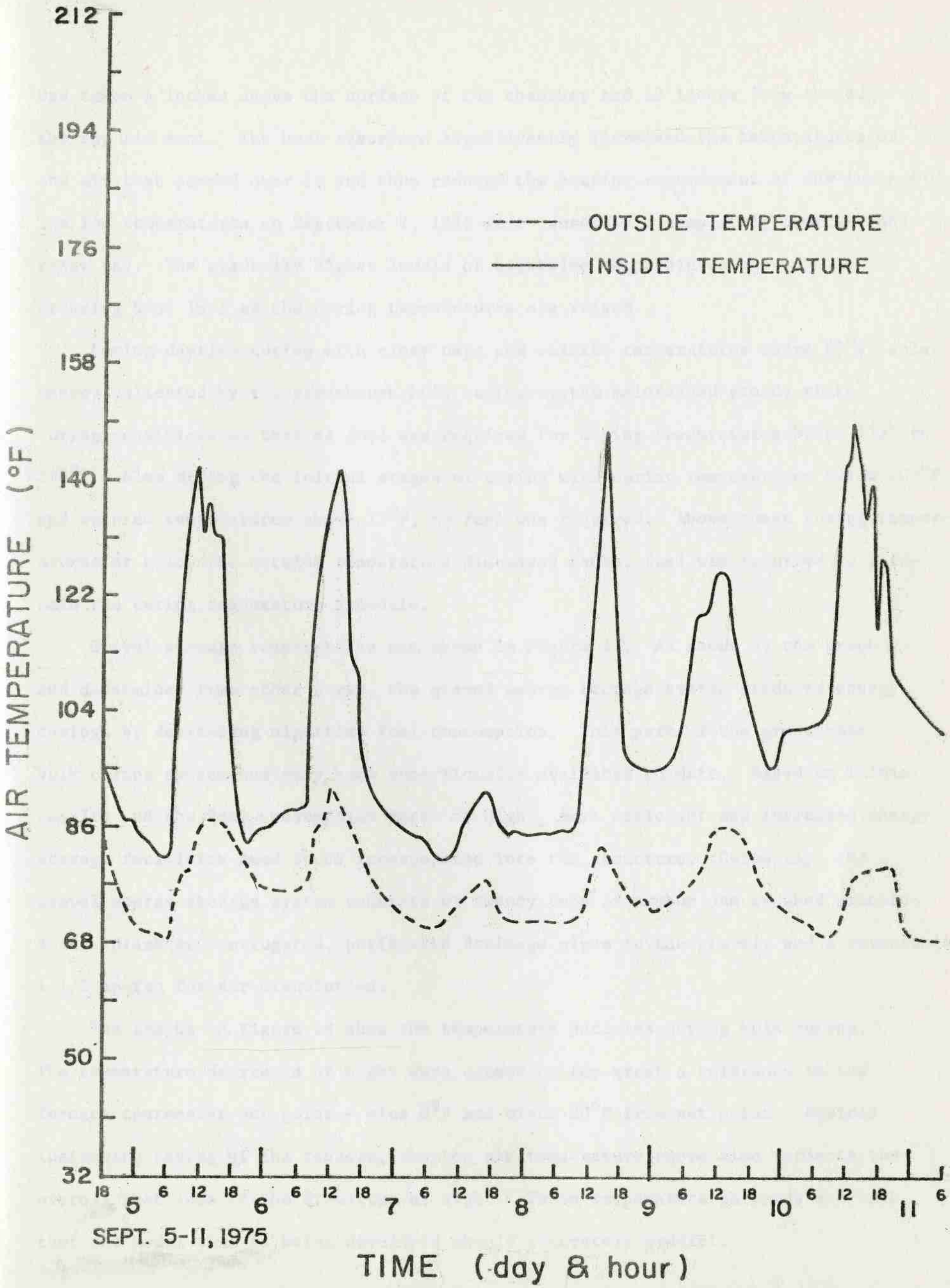

Figure 16. Air temperature increases due to solar energy collection during bulk curing of tobacco.

was taken 5 inches above the surface of the absorber and 12 inches from the edge of the top air duct. The heat absorbers significantly increased the temperatures of the air that passed over it and thus reduced the heating requirement of the furnace. The low temperatures on September 7, 1975 were caused by a completely overcast and rainy day. The gradually higher levels of nighttime temperatures show the increasing heat loss as the curing temperatures are raised.

During daytime curing with clear days and outside temperatures above $85^{o}F$, solar energy collected by the greenhouse bulk curing system maintained steady state curing conditions so that no fuel was required for curing temperatures below 115^{o} to $120^{o}F$. Also during the initial stages of drying with curing temperatures below $100^{o}F$ and outside temperatures above $72^{o}F$, no fuel was required. Above these curing temperatures or below the outside temperature discussed above, fuel was required to maintain the curing temperature schedule.

Gravel storage temperatures are shown in Figure 17. As shown by the graph and determined from other cures, the gravel energy storage system produced energy savings by decreasing nighttime fuel consumption. This part of the greenhouse bulk curing system has only been superficially evaluated to date. Based on initial results and the fuel consumption rates at night, more efficient and increased energy storage facilities need to be incorporated into the structure. Currently, the gravel energy storage system consists of twenty tons of number one crushed granite; 8 inch diameter, corrugated, perforated drainage pipes in the gravel; and a reversable 1 1/2 hp fan for air circulation.

The graphs in Figure 18 show the temperature patterns during bulk curing. The temperature decreases at night were caused by too great a tolerance in the furnace thermostat set point - plus $0^{o}F$ and minus $20^{o}F$ from set point. Besides indicating drying of the tobacco, the top air temperature curve also reflects the overall heat loss of the structure at night. These temperature patterns are ones that the model that is being developed should accurately predict.

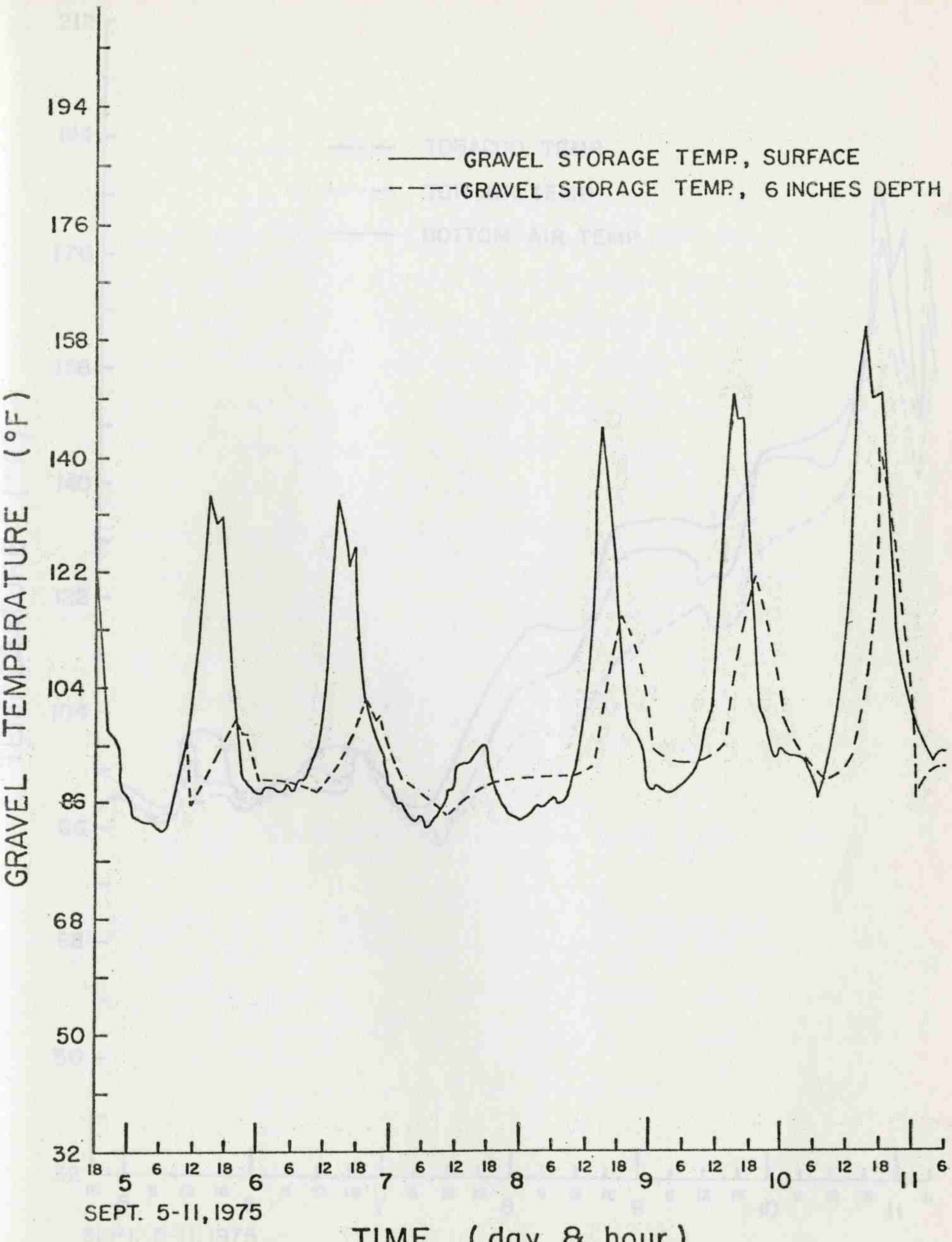

Figure 17. Gravel storage temperature changes indicating solar energy storage during bulk curing.

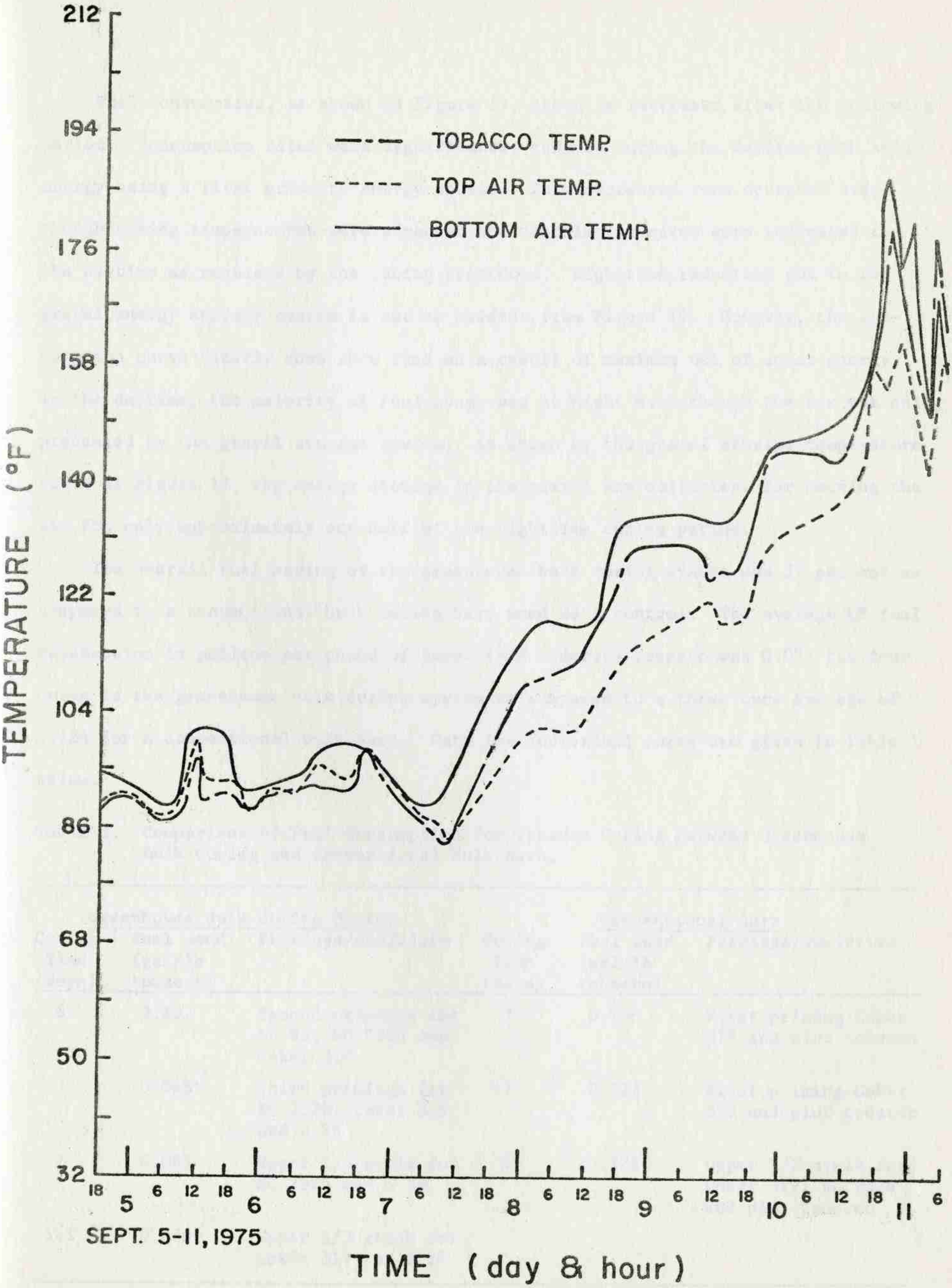

Figure 18. Temperature patterns during bulk tobacco curing with solar energy.

Fuel consumption, as shown in Figure 19, steadily increased after the yellowing period. Consumption rates were significantly reduced during the daytime with solar energy being a first priority energy source. This decreased rate occurred even though curing temperatures were advanced and ventilation rates were increased in the daytime as required by the curing procedure. Nighttime reduction due to the gravel energy storage system is not as evident from Figure 19. However, the consumption curve clearly does show that as a result of maximum use of solar energy in the daytime, the majority of fuel usage was at night even though the air was being preheated by the gravel storage system. As shown by the gravel storage temperature curve of Figure 17, the energy storage in the gravel was sufficient for heating the air for only approximately one-half of the nighttime curing period.

The overall fuel saving of the greenhouse bulk curing system was 37 percent as compared to a conventional bulk curing barn used as a control. The average LP fuel consumption in gallons per pound of cured (and ordered) tobacco was 0.077 for four cures in the greenhouse bulk curing system as compared to a three cure average of 0.124 for a conventional bulk barn. Data for individual cures are given in Table 1 below.

Table 1. Comparison of Fuel Consumption for Tobacco Curing Between Greenhouse Bulk Curing and Conventional Bulk Barn.

Greenhouse Bulk Curing System			Conventional Barn		
Curing Time (days)	Fuel used (gal/lb tobacco)	Primings/varieties	Curing Time (days)	Fuel used (gal/lb tobacco)	Primings/varieties
6	0.107	Second primings for NC 95, NC 2326 and Coker 319	7	0.136	First priming Coker 319 and plot tobacco
7	0.068	Third primings for NC 2326, Coker 319 and G 28	7	0.111	First priming Coker 319 and plot tobacco
7	0.065	Upper 1/3 stalk for NC 2326 and G 28	6	0.126	Upper 1/2 stalk for Coker 319, NC 2326 and plot tobacco
6.5	0.076	Upper 1/3 stalk for Coker 319 and G 28			

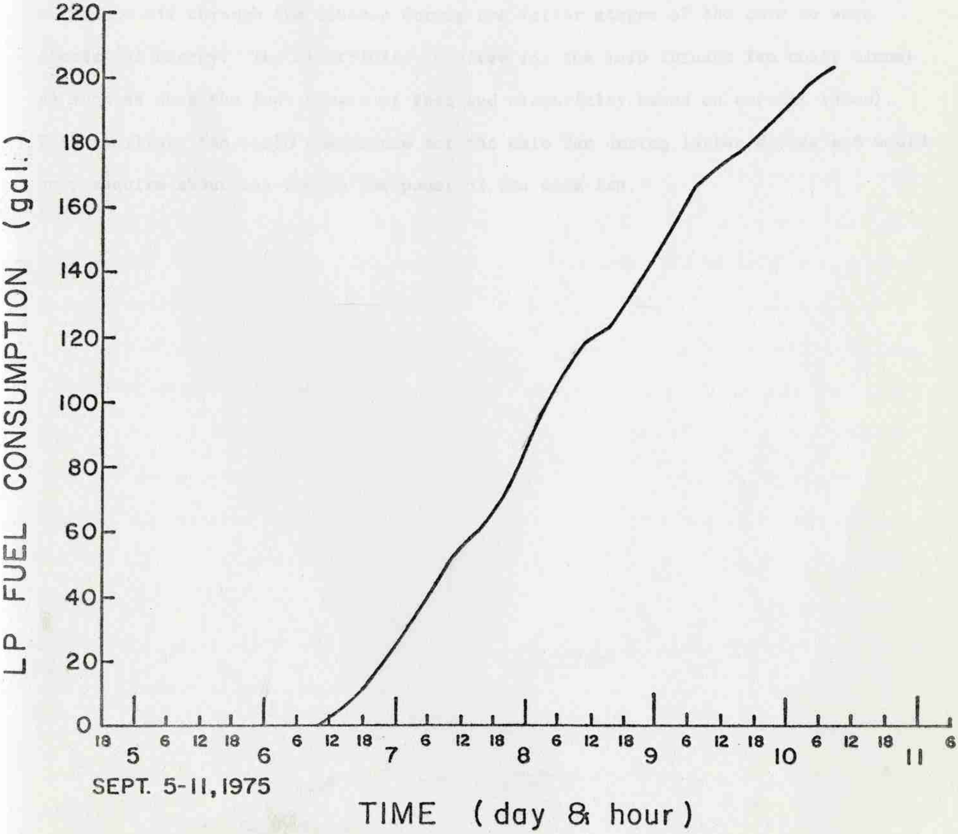

Figure 19. Fuel consumption in greenhouse bulk curing and drying system for bulk curing of tobacco using solar energy.

Cures in each barn were similarly managed and occurred over approximately the same overall time periods. The lower stalk tobacco and surface moisture resulting from harvesting in the rain caused the fuel consumption of the first cure in the greenhouse bulk curing system to be appreciably higher than other cures.

Another feature to be considered in the greenhouse bulk curing and drying system during tobacco curing is using the auxiliary gravel storage system fan to circulate air through the tobacco during the latter stages of the cure to save electrical energy. The electricity required for the main furnace fan costs almost as much as does the fuel (Costs of fuel and electricity based on current rates). This auxiliary fan could substitute for the main fan during latter drying and would only require about one-fourth the power of the main fan.

GREENHOUSE OPERATION OF GREENHOUSE BULK CURING AND DRYING SYSTEM

The structure was converted to the greenhouse mode of operation in October, 1975. Potted Klanchoe flowers were grown in it from November, 1975 to March, 1976 (Figure 20). The automatic temperature and watering, discussed in a previous section, produced an excellent crop of flowers. It was estimated that a flowering crop such as the Klanchoes would provide between $700 to $800 income in a 4 month growing period.

Data for the air temperature distribution, air flows, energy storage in gravel, fuel consumption, and solar radiation are now being analyzed for a thorough evaluation of the greenhouse operation of the greenhouse bulk curing and drying system. Initial indications are that the collection, storage, and utilization of solar energy resulted in approximately a 10% fuel savings.

With the removal of the flowers in March, 1976, the portable frames with four perforated sheet metal layers were placed in the greenhouse for tobacco seedling production. An automated misting system was added. Tobacco seeds were placed in the seedling growing and handling trays, and the trays were put on three layers. The seeding was done in April 1976, and the seedlings were removed in May 1976.

Excellent germination rates of 95-97% were obtained on each layer (Figure 21). Uniform growth occurred through the third week at which time the seedlings were damaged by over-fertilization. Additionally, light level variation with each layer and within each layer contributed to non-uniform growth. This lighting difficulty can be solved either by adding artificial lighting or by rotating the layers.

Figure 20. Greenhouse bulk curing and drying system during greenhouse operation for growing flowers.

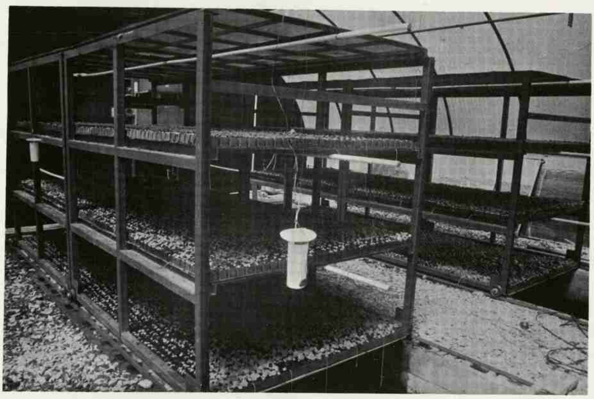

Figure 21. Tobacco transplant production in greenhouse bulk curing and drying system.

SYSTEM ANALYSIS AND COMPUTER SIMULATION

Thermal Circuit Development (5)

Electrical systems are analogous to many other systems such as mechanical systems, hydraulic systems, thermal systems, etc. Huang (7,8,9) has illustrated systems analogies and the mathematical interpretation of several biological and physical systems often encountered in the field of agricultural engineering. Any system which has electrical analogies may be simulated with circuit network without formulating the mathematical model and solving the resulting mathematical equations. Electrical analogies to a thermal system are given in Table 2.

Table 2. Analogies in Thermal and Electrical Systems

Thermal System	Electrical System
Temperature T	Voltage
Heat Flow Q	Current
Thermal Capacitance C	Capacitance
Thermal Conductivity K	Conductance
Thermal Resistance R	Resistance

Three modes of heat transfer-conduction, convection, and radiation-were considered in working out the thermal circuits representing the solar drying system.

Conduction:

The heat transfer in a medium by conduction can be expressed as:

$$Q = -KA \frac{dT}{dX} \qquad (1)$$

where $\quad Q$ = heat flow rate (heat flux)(Btu/hr)

K = thermal conductivity (Btu/hr ft^{o}F)

A = cross-sectional area perpendicular to the heat flow (ft^2)

$\frac{dT}{dX}$ = temperature gradient (^{o}F/ft), or the rate of temperature T change with respect to distance X in the direction of heat flow.

Consider the steady-state heat flow through a conductor of length L, cross-sectional area A, and assume K is independent of T. Eq. (1) can be rewritten as:

$$Q = KA \frac{T_1 - T_2}{L} \tag{2}$$

The thermal resistance R, which is analogous to electrical resistance, can then be expressed by:

$$R = \frac{L}{KA} \left(\frac{^{o}F}{Btu/hr}\right) \tag{3}$$

Thermal capacity, or the heat necessary to cause unit change in temperature of the mass, may be defined as:

$$C = \frac{Q}{T_f - T_i} = \frac{\int_{T_i}^{T_f} C_p \gamma dT}{T_f - T_i} \tag{4}$$

where Q = thermal energy required to raise the temperature of a given mass from T_i to T_f

C_p = specific heat capacity (Btu/lb^{o}F)

γ = density (lb/ft^3)

T_i = initial temperature (^{o}F)

T_f = final temperature (^{o}F)

If C_p and γ are constant over the temperature interval considered or if appropriate mean values of these quantities are used, Eq. (4) may be written as:

$$C = C_p \gamma V (Btu/^{o}F) \tag{5}$$

where V = volume of the mass (ft^3)

Convection:

The heat transfer between air and a solid surface can be expressed as:

$$Q_c = h_c A \, (T_s - T_a) \tag{6}$$

where Q_c = rate of heat flow (Btu/hr)

h_c = convection coefficient (Btu/hr ft^2 $^{\circ}$F)

A = cross-sectional area perpendicular to heat flow (ft^2)

T_s = temperature of the surface ($^{\circ}$F)

T_a = temperature of the air ($^{\circ}$F)

The convection thermal resistance R_c can then be expressed as:

$$R_c = \frac{1}{h_c A} \left(\frac{^{\circ}F}{Btu/hr}\right) \tag{7}$$

Radiation:

Radiation exchange occurs through a separating space between objects as a result of their temperatures. If an enclosure has m surface and all surfaces are gray and opaque, diffuse and uniform in temperature, and their reflective and emissive properties are constant over all surfaces, the net energy exchange at a particular surface boundary (i) may then be expressed as (4,14).

$$(q_{net})_i = \frac{A_i \varepsilon_i}{1-\varepsilon_i} \left[R_i - (E_b)_i\right]$$

$$= \frac{R_i - (E_b)_i}{\dfrac{1-\varepsilon_i}{A_i \varepsilon_i}} \tag{8}$$

where q_{net} = net energy exchange (Btu/ft^{2}hr)

R = radiosity or total radiation which leaves a surface per unit time and per unit area (Btu/ft^{2}hr)

E_b = blackbody emissive power (Btu/ft^{2}hr)

ε = emissivity of a surface

A = area of a surface (ft^2)

In Eq. (8), $\frac{1-\varepsilon}{A\varepsilon}$ is considered as "surface resistance" to radiation heat transfer. The net energy can also be expressed as:

$$(q_{net})_i = \sum_{n=1}^{m} F_{in}A_i\ (R_n - R_i)$$

$$= \sum_{n=1}^{m} \frac{R_n - R_i}{\frac{1}{F_{in}A_i}} \tag{9}$$

where

F_{in} = shape factor or fraction of energy leaving surface i which reaches surface n

$F_{in}A_i = F_{ni}A_n$ (by the law of reciprocity)

The term $\frac{1}{F_{in}A_i}$ is considered as "space resistance" to radiation heat transfer. From Eqs. (8) and (9) an energy balance at R_i or radiation at the i^{th} surface would result in

$$\frac{R_i - (E_b)_i}{\frac{1-\varepsilon_i}{A_i\varepsilon_i}} = \sum_{n=1}^{m} \frac{R_n - R_i}{\frac{1}{A_iF_{in}}} \tag{10}$$

An equation similar to Eq. (10) may be written for each of the (m) surfaces resulting in a closed resistance network representing the system of (m) radiating surfaces. Figure 22(a) shows the thermal network of radiation at the i^{th} surface, in which E_b and R are proportional to the fourth power of their absolute temperatures. In order to use such a network in the thermal circuit representing the conduction paths of a heat transfer system, it is desirable to adjust the resistors so that a first power temperature potential at each of the (E_b) nodes would result in the same heat or current flow through all of the resistors. In order to determine the proper adjustment of each resistor, consider a path through the network between $(E_b)_i$ and $(E_b)_n$ or:

$$\frac{t_i - t_n}{NR} = \frac{(E_b)_i - (E_b)_n}{R} \tag{11}$$

where

R = sum of all resistors between $(E_b)_i$ and $(E_b)_n$

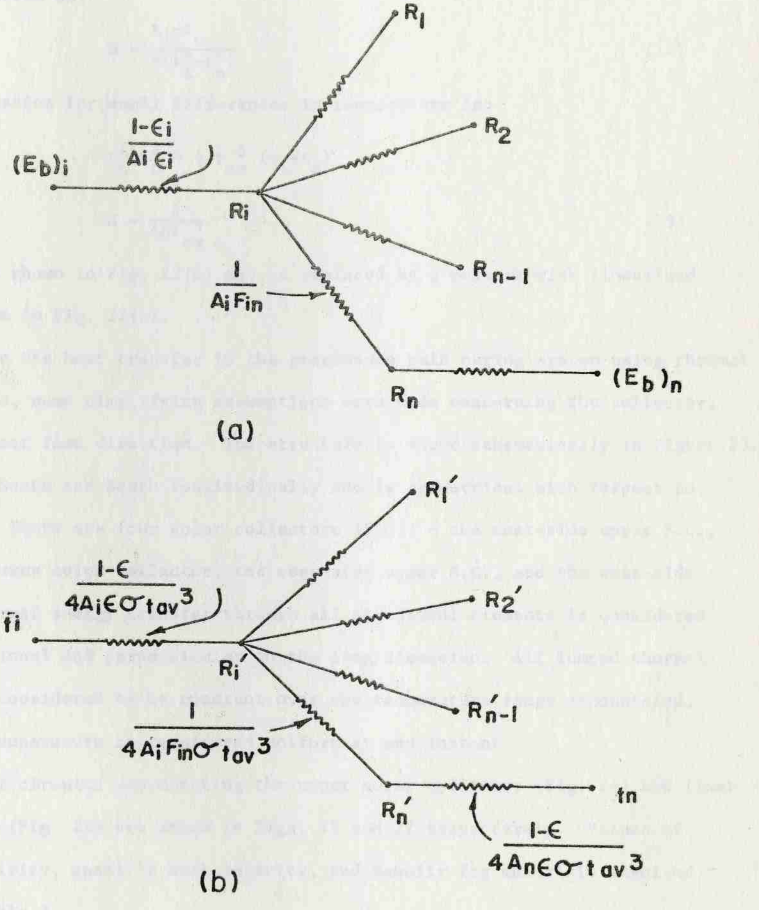

Figure 22. Radiation thermal network.

N = adjustment in resistance to linearize the potential

t_i and t_n = absolute temperatures at i and n surface respectively.

Since $(E_b)_i = \sigma t_i^4$ and $(E_b)_n = \sigma t_n^4$, where σ is the Stefan-Boltzmann constant, Eq. (11) can then be written as:

$$N = \frac{t_i - t_n}{\sigma(t_i^4 - t_n^4)} \qquad (12)$$

A good approximation for small differences in temperature is:

$$t_i^4 - t_n^4 = 4\ t_{av}^{\ 3}\ (t_i - t_n)$$

Then,

$$N = \frac{1}{4\sigma t_{av}^{\ 3}} \qquad (13)$$

and the network shown in Fig. 22(a) may be replaced by a network with linearized potentials shown in Fig. 22(b).

To describe the heat transfer in the greenhouse bulk curing system using thermal circuit analysis, some simplifying assumptions were made concerning the collector, air flow, and heat flow direction. The structure is shown schematically in Figure 23. It is directed North and South longitudinally and is symmetrical with respect to East and West. There are four solar collectors (S.C.) - the east-side upper S.C., the east-side lower solar collector, the west-side upper S.C., and the west-side lower S.C. Thermal energy transfer through all structural elements is considered to be unidirectional and perpendicular to the long dimension. All lumped thermal properties are considered to be constant over the temperature range encountered, and the space temperature is considered uniform at any instant.

The thermal circuits representing the upper solar collector (Fig. 24) and lower solar collector (Fig. 26) are shown in Figs. 25 and 27 respectively. Values of thermal conductivity, specific heat capacity, and density for materials involved are given in Table 3.

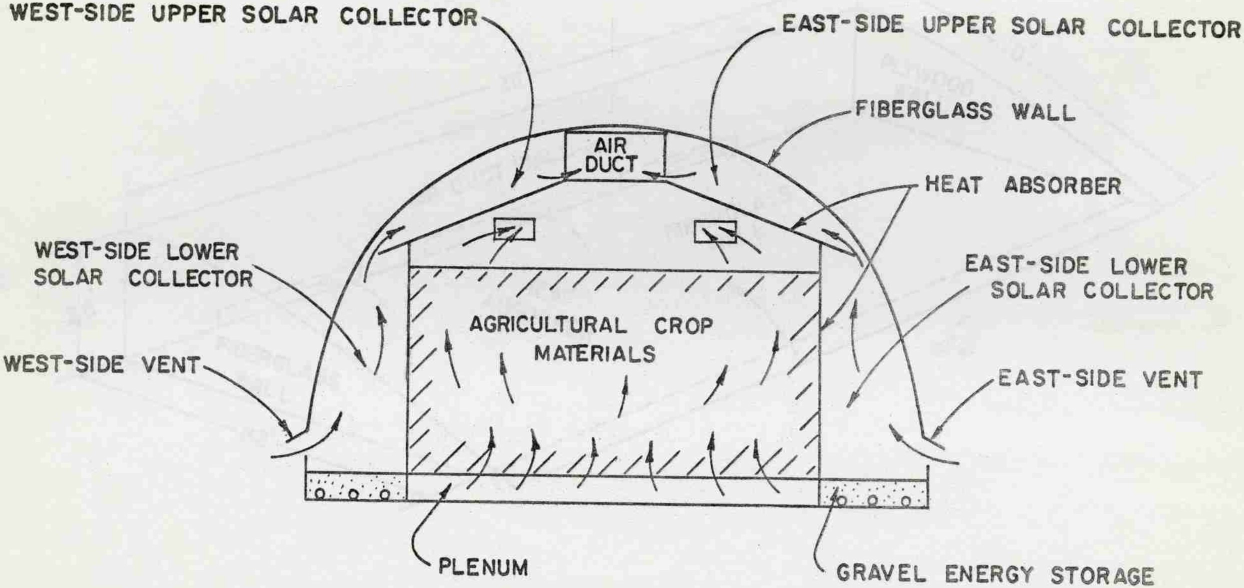

Figure 23. Schematic cross-sectional view of greenhouse bulk curing and drying system.

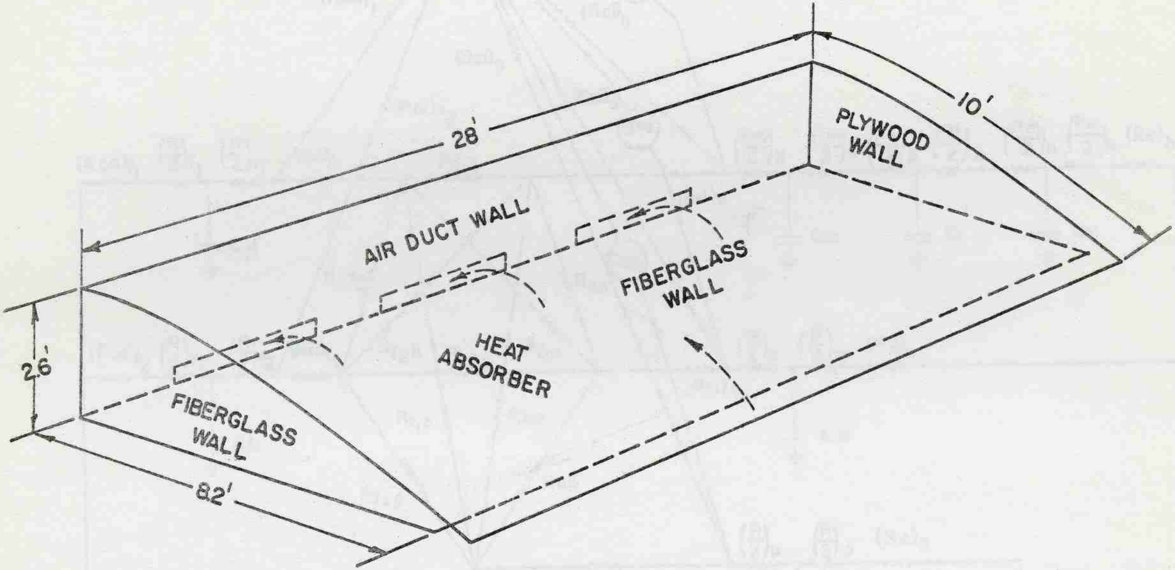

Figure 24. Schematic diagram and dimensions of upper solar collector.

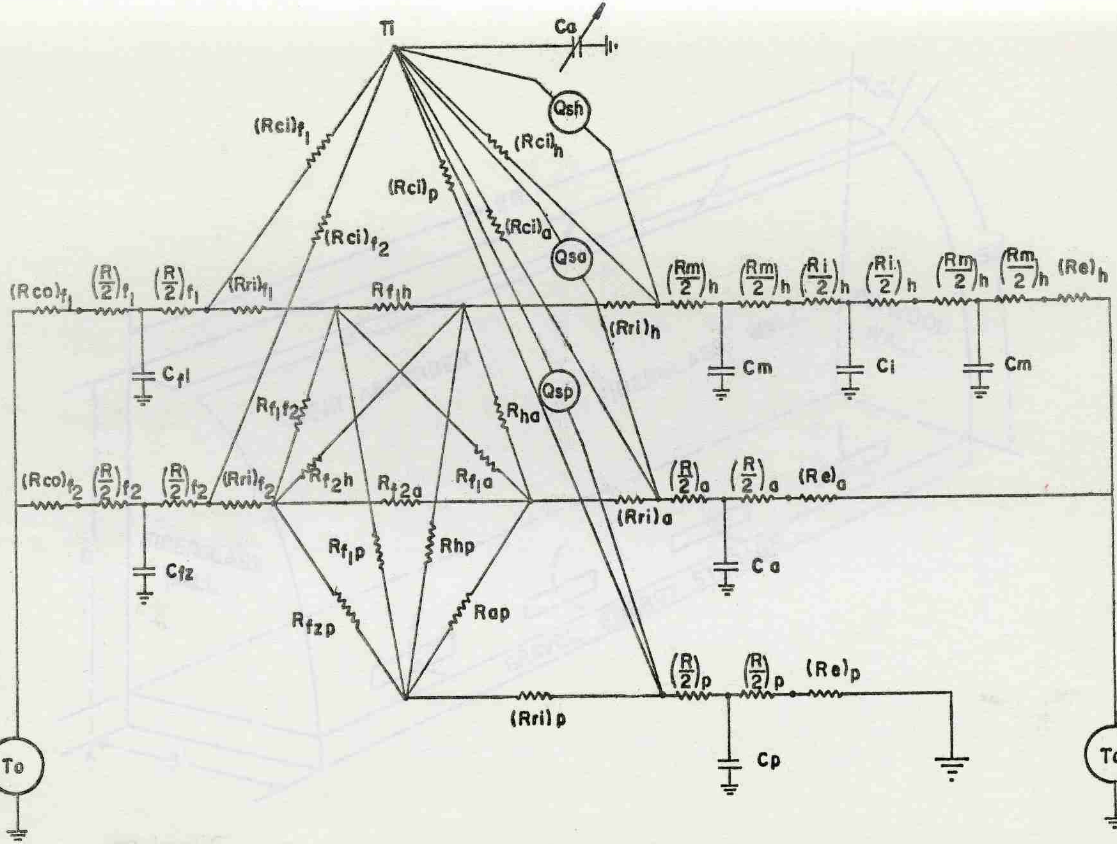

Figure 25. Thermal circuit representing upper solar collector.

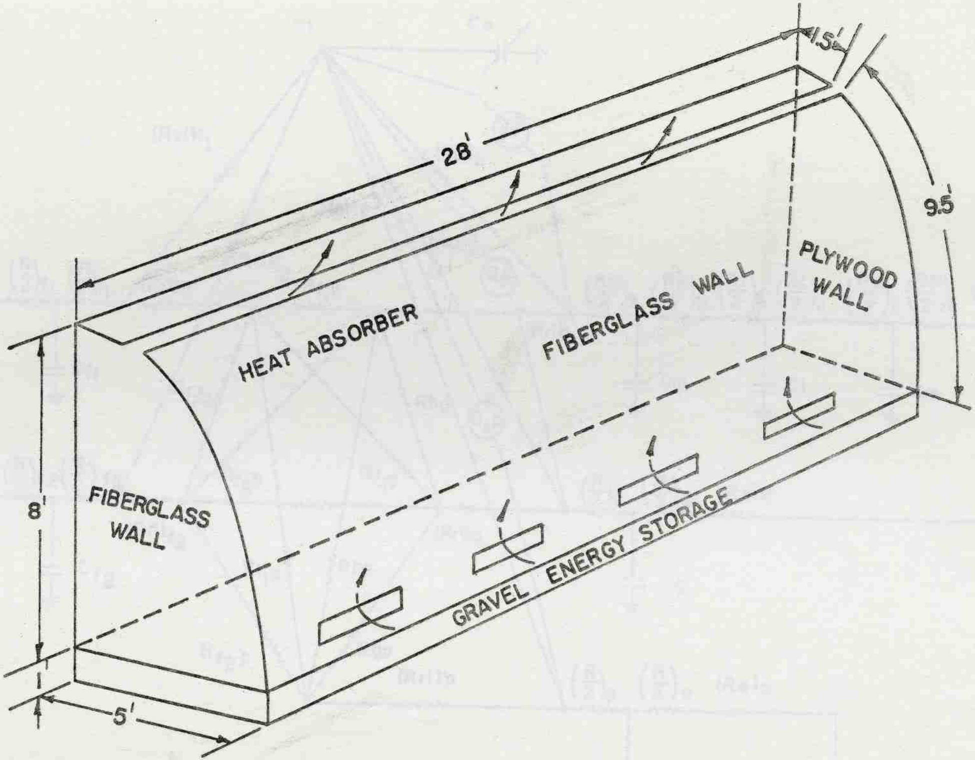

Figure 26. Schematic diagram and dimensions of lower solar collector.

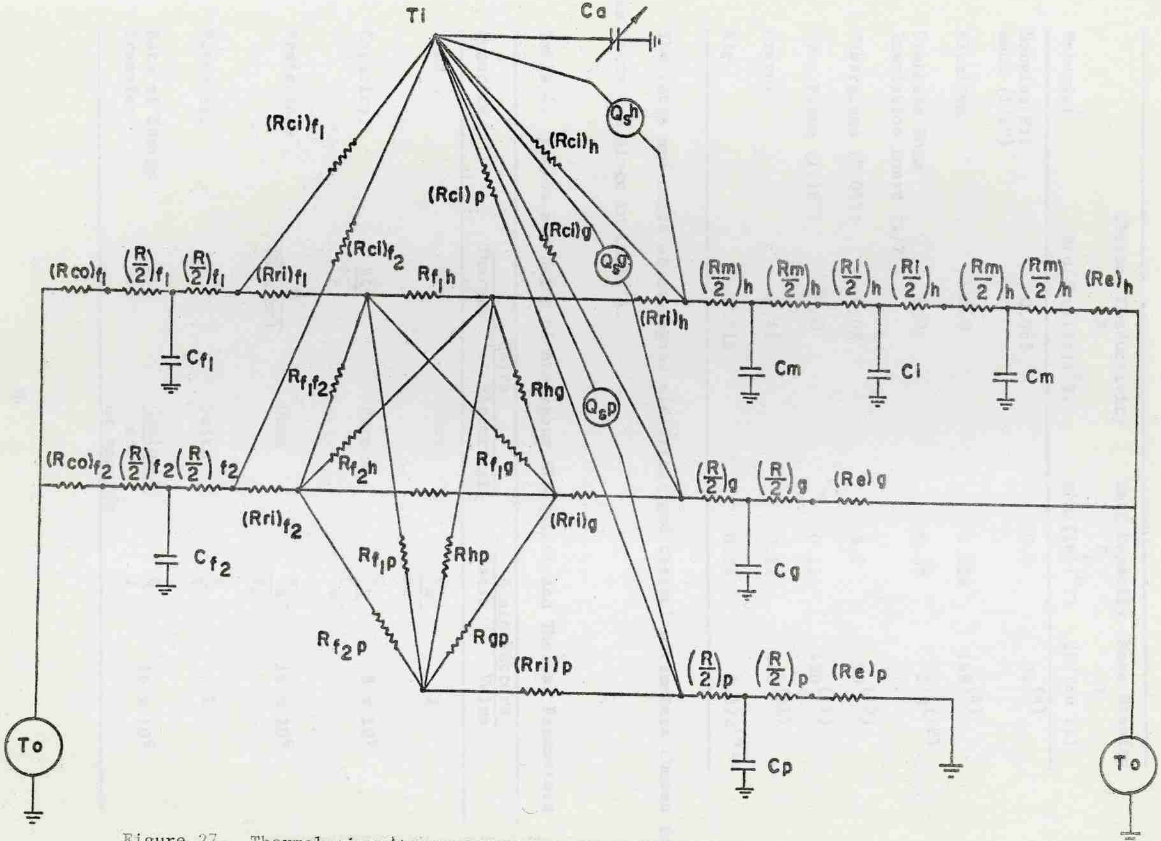

Figure 27. Thermal circuit representing lower solar collector.

Table 3. Thermal Properties of Materials Used

Material	Thermal Conductivity K Btu/(hr)(ft)(^oF)	Heat Capacity C_ρ Btu/(lb)(^oF)	Mass Density γ lb/(cu ft)
Douglas Fir Wood (1/2")	0.065	0.5	34 (4)
Aluminum	118.0	0.214	169 (4)
Urethane Foam Insulation Board (1/2")	0.01	0.35	2.0 (12)
Fiberglass (0.04")	0.02	0.2	90 (12)
Iron Plate (1/16")	34.0	0.11	490 (11)
Gravel	0.42	0.22	120 (11)
Air	0.016	0.24	0.072 (4)

The ratio and units of analogous electrical and thermal parameters chosen for this study are given in Table 4.

Table 4. Ratios and Units of Analogous Electrical and Thermal Parameters

Quantity	Units		Scale Factors	
	Thermal	Electrical	Ratio	Value
Time	hrs	sec	$\frac{\theta_{e'}}{\theta t}$	2
Capacity	$\frac{Btu}{^oF}$	Farads	$\frac{C_t}{C_{e'}}$	8×10^6
Resistance	$\frac{^oF}{(Btu/hr)}$	Ohms	$\frac{R_{e'}}{R_t}$	16×10^6
Potential	^oF	Volts	$\frac{E}{T}$	1
Rate of Energy Transfer	$\frac{Btu}{hr}$	$\frac{Coulombs}{sec}$ or Amperes	$\frac{Q}{I}$	16×10^6

The symbols used in Figs. 25, 27 and Table 4 are defined as follows:

Symbols	Subscripts
R = conduction resistance	f_1 = tilted fiberglass wall
R_{co} = outside convection resistance	f_2 = vertical fiberglass wall
R_{ci} = inside convection resistance	h = heat absorber
R_{ri} = inside 'surface' radiation resistance	d = top air duct
R_{xy} = inside 'space' radiation resistance	g = gravel energy storage
C = capacitor	p = plywood wall
T_i = inside air temperature	m = aluminum foil
T_o = outside air temperature	i = insulating material
Q_s = solar radiation input	a = air space
R_e = equivalent resistance ($\sim 5000 \times 10^3$ ohms)	e' = electrical circuit element
θ = time	t = thermal circuit element
E = constant electrical potential	
T = temperature	
Q = heat flux	
I = electric current	

A summary of the conduction path resistors and capacitors for the walls of the solar collector is given in Table 5.

Table 5. Values of Solar Collector Wall Conduction Path Resistors and Capacitors

		Conduction Resistance ($R \times 10^3$ ohms)	Capacitor ($C \times 10^{-6}$ farads)
	Heat Absorber (h)		
	Aluminum Foil (m)	10^{-4}	0.16
	Insulation Board (i)	289.7	0.84
Upper Solar Collector	Tilted Fiberglass Wall (f_1)	10.0	2.1
	Vertical Fiberglass Wall (f_2)	157.4	0.13
	Air Duct Wall (d)	0.04	2.61
	Plywood Wall (p)	580.1	1.57

Table 5. Cont'd

		Conduction Resistance ($R \times 10^3$ ohms)	Capacitor ($C \times 10^{-6}$ farads)
	Heat Absorber (h)		
	Aluminum Foil (m)	10^{-4}	0.17
	Insulation Board (i)	291.4	0.8
Lower Solar Collector	Tilted Fiberglass Wall (f_1)	10.6	1.97
	Vertical Fiberglass Wall (f_2)	78.7	0.26
	Plywood Wall (p)	290.0	3.13
	Gravel Energy Storage (g)	1400.0	486.1

For the evaluation of convection resistance between the exposed surfaces and the air mass, a convection coefficient h_c was estimated. The values of h_c were calculated from the equations in ASHRAE GUIDE (1) and were adjusted to take into account the roughness of the surfaces. For a given surface in air, the convective resistance is influenced mainly by the air velocity over the surface.

The wind velocity on October 7, 1975 was between 100-200 fpm during the day and less than 50 fpm during the night. Hence, the values of outside h_c were estimated as 1.0 and 0.7 Btu/hr ft^2 ^{o}F for the day and night respectively. There was no air movement inside the solar collector on October 7, 1975. The values of inside h_c were estimated as 0.5, 0.6 and 0.7 Btu/hr ft^2 ^{o}F for vertical, horizontal and tilted surfaces respectively, based on free convection. A summary of convection resistances based on the above convection coefficients for the upper solar collectors is given in Table 6. The wind velocity on September 5, 1975 was between 200-500 fpm during the day and less than 50 fpm during the night. Hence, the values of outside h_c were estimated as 1.4 or 0.7 Btu/hr ft^2 ^{o}F for day and night respectively. Even though there was air movement within the solar collector on September 5, 1975, its velocity was small. Therefore, the values of inside h_c were estimated as 0.5, 0.7

and 0.4 Btu/hr ft^2 ^oF for vertical, horizontal and tilted surfaces respectively. A summary of convection resistances for the upper and lower solar collector based on the above convection coefficients is given in Table 7.

Table 6. Convection Resistances for Upper Solar Collector (Case I)

	Outside Convection Resistance (R_{co} x 10^3 ohms)		Inside Convection Resistance (R_{ci} x 10^3 ohms)
	Day	Night	
Heat Absorber (h)	-	-	116.1
Tilted Fiberglass Wall (f_1)	57.6	82.4	144.1
Vertical Fiberglass Wall (f_2)	904.9	1292.8	1801.1
Air Duct Wall (d)	-	-	430.1
Plywood Wall (p)	-	-	1801.1

Table 7. Convection Resistances for Solar Collectors (Case II)

		Outside Convection Resistance (R_{co} x 10^3 ohms)		Inside Convection Resistance (R_{ci} x 10^3 ohms)
		Day	Night	
Upper Solar Collector	Heat Absorber (h)	-	-	99.4
	Tilted Fiberglass Wall (f_1)	41.2	82.4	144.1
	Vertical Fiberglass Wall (f_2)	646.4	1292.8	1801.1
	Air Duct Wall (d)	-	-	430.1
	Plywood Wall (p)	-	-	1801.1
Lower Solar Collector	Heat Absorber (h)	-	-	140.0
	Tilted Fiberglass Wall (f_1)	43.4	86.8	152.0
	Vertical Fiberglass Wall (f_2)	323.1	646.2	904.7
	Plywood Wall (p)	-	-	904.7
	Gravel Energy Storage (g)	-	-	184.3

The corresponding capacitors for simulating various air velocities inside the solar collector are given in Table 8.

Table 8. Values of C_a

Collector-Air Flow Rate (cfm)	C_a (x 10^{-6} farads) Upper Solar Collector	Lower Solar Collector
0	1.07	2.14
180	23.2	23.2
300	38.8	38.8
340	44.1	44.1

Radiation exchange within the solar collector was represented by a similar resistance network as shown in Fig. 22(b) which applied to five surfaces. The shape factors were computed with the aid of equations and charts (4,14). An average surface temperature of 610 ^{o}R and emissivity of 0.95 were used in the evaluation of the network resistances. A summary of network resistances is given in Table 9.

Table 9. Inside Radiation Exchange Network Resistances (R x 10^3 ohms)

Upper Solar Collector	$(R_{ri})_{f1}$	2.4	R_{f1h}	70.3	R_{f1d}	230.5
	$(R_{ri})_{f2}$	37.5	R_{hd}	445.0	R_{f2h}	2739.3
	$(R_{ri})_{h}$	2.9	R_{dp}	5635.7	R_{f1p}	1135.1
	$(R_{ri})_{d}$	8.9	R_{f2p}	71221.7	R_{hp}	2735.5
	$(R_{ri})_{p}$	37.5	R_{f1f2}	1187.1	R_{f2d}	5478.6
Lower Solar Collector	$(R_{ri})_{f1}$	1.8	R_{f1h}	67.6	R_{f1g}	135.2
	$(R_{ri})_{f2}$	16.1	R_{hg}	236.5	R_{f2h}	956.2
	$(R_{ri})_{h}$	2.5	R_{gp}	1223.9	R_{f1p}	742.6
	$(R_{ri})_{g}$	3.9	R_{f2p}	16998.7	R_{hp}	756.2
	$(R_{ri})_{p}$	16.1	R_{f1f2}	742.6	R_{f2p}	1223.9

The solar radiation energy (Q_s, Btu/hr) absorbed by various surfaces of the solar collector can be evaluated with the following equations:

$$Q_s = (q)(\text{coeff. of transparency of the fiberglass wall, 0.75})(\text{absorptivity of the surface})(\text{area of the surface}) \quad (14)$$

$$q = \frac{\text{Cos}\,\theta}{\text{Sin}\,\beta}(H_t - H_d) + \frac{1}{2}(1+\text{Cos}\phi)\,H_d + \frac{1}{2}(1-\text{Cos}\phi)\,\rho H_t \quad (15)$$

where q = total radiation incident upon tilted surface per unit time per unit area (Btu/(hr)(ft^2))

H_t = total radiation incident upon a horizontal surface per unit time per unit area (Btu/(hr)(ft^2))

H_d = diffuse radiation incident upon a horizontal surface per unit time per unit area (Btu/(hr)(ft^2))

θ = incidence angle of solar energy upon the tilted surface

β = altitude angle of the sun

ϕ = tilt angle of the surface from the horizontal

ρ = ground surface reflectance

The solar radiation absorptivity of various surfaces is listed in Table 10. The incidence and altitude angles are determined from the following equations:

$$\text{Cos}\,\theta = \text{Cos}\,\beta\,\text{Cos}\,\psi\,\text{Sin}\,\phi + \text{Sin}\,\beta\,\text{Cos}\,\phi \quad (16)$$

$$\text{Sin}\,\beta = \text{Cos}\,L\,\text{Cos}\,H\,\text{Cos}\,D + \text{Sin}\,L\,\text{Sin}\,D \quad (17)$$

where

ψ = wall solar azimuth angle and is the angle in a horizontal plane between the surface's azimuth and the sun's azimuth

L = latitude

H = hour angle

D = sun's declination

Table 10. Solar Radiation Absorptivities of Various Surfaces (4)

Surface	Absorptivity for Solar Radiation
Heat Absorber	0.95
Air Duct Wall	0.95
Plywood Wall	0.95
Gravel Energy Storage	0.70

Circuit Simulation Analysis and Verification (5)

For the thermal circuit analysis, two cases of the thermal behavior of the solar collector were investigated:

Case I. No air movement within the solar collector, i.e. free convection within the solar collector.

Case II. Air movement within the solar collector. A 7.5 hp fan moved the air within the solar collector. The air velocity was controlled by the opening of the vents (Fig. 23).

For the case of no air movement within solar drying system, the circuit shown in Fig. 25 and the corresponding values of the resistance and capacitance given in Tables 5, 7, 8 and 9 were used. The input outside air temperature potential and the solar radiation on a horizontal surface on Oct. 7, 1975 are shown in Figs. 28 and 29 respectively. The solar radiation absorbed by the surfaces of heat absorbers, top air duct wall, and plywood wall were evaluated with the aid of Eqs. (14) and (15). In Eq. (15), the ground surface reflectance was assumed to be 0.2 because the surrounding ground was covered with vegetation (1).

For the case of air movement within the solar drying system, the collector air flow rate was forced up to 300 ft^3/min from 9:00 AM to 12:00 noon, 340 ft^3/min from 12:00 noon to 9:00 PM, and 180 ft^3/min for the rest of hours on Sept. 5, 1975. The circuits used

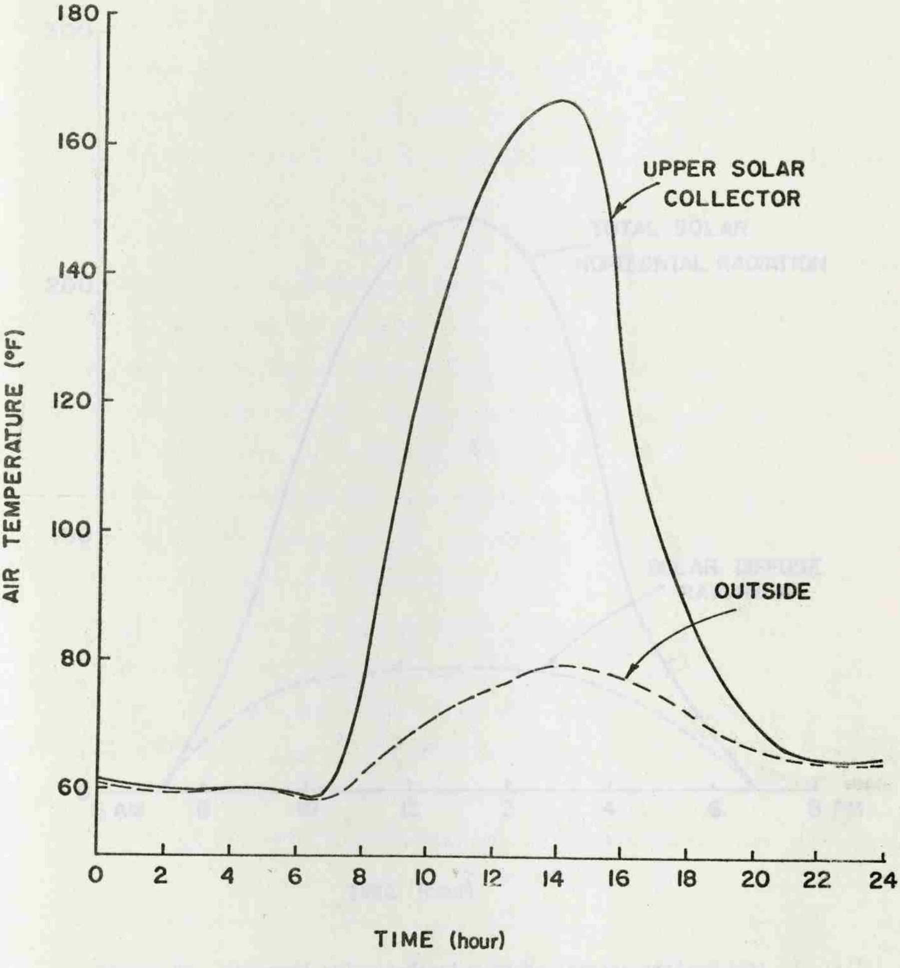

Figure 28. Diurnal variation of outside air and east-side collector air temperatures for case of no air movement (Oct. 7, 1975).

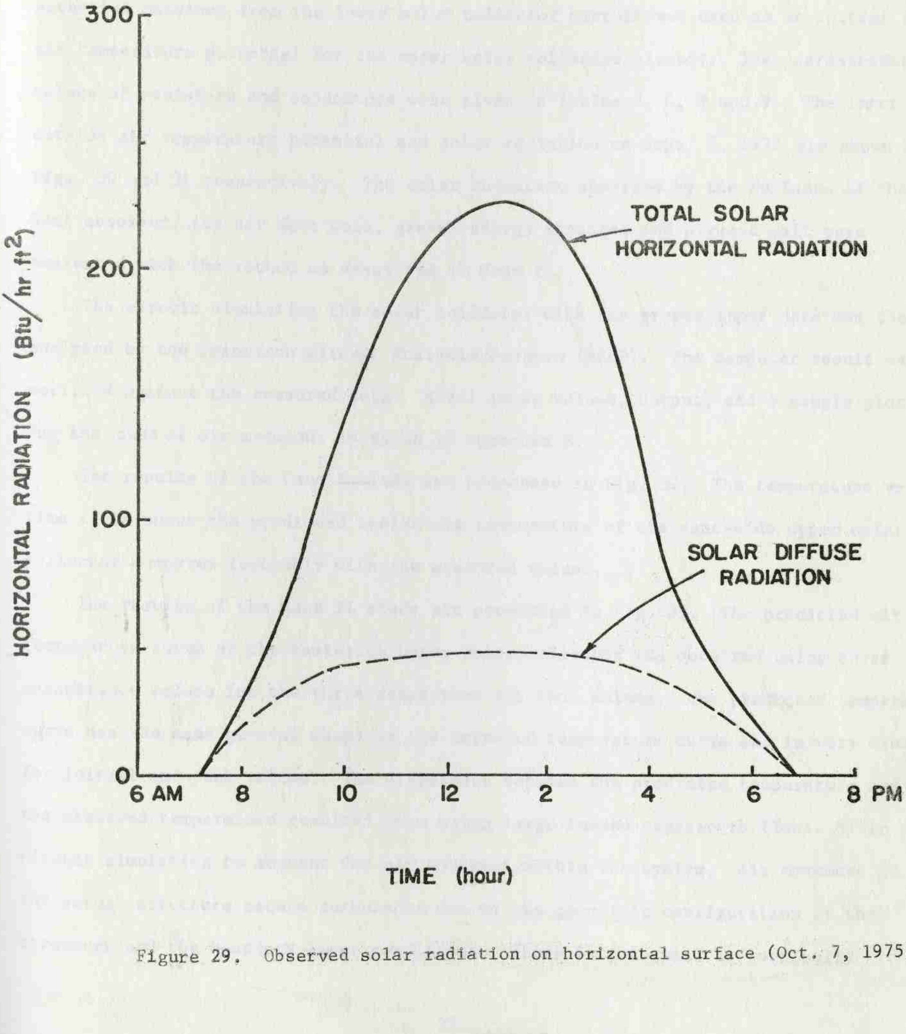

Figure 29. Observed solar radiation on horizontal surface (Oct. 7, 1975).

were shown in Figs. 25 and 27. The moving air was first heated in the lower solar collector and then entered the upper solar collector where the air was heated again before it entered the top air duct. Therefore, for Case II the inside air temperature potential obtained from the lower solar collector circuit was used as an initial inside air temperature potential for the upper solar collector circuit. The corresponding values of resistors and capacitors were given in Tables 5, 6, 8 and 9. The input outside air temperature potential and solar radiation on Sept. 5, 1975 are shown in Figs. 30 and 31 respectively. The solar radiation absorbed by the surfaces of the heat absorber, top air duct wall, gravel energy storage, and plywood wall were evaluated with the method as described in Case I.

The circuit simulating the solar collector with the proper input data was then analyzed by the Princeton Circuit Analysis Program (PCAP). The computer result was verified against the measured data. Nodal input values, output, and a sample plot for the case of air movement is given in Appendix B.

The results of the Case I study are presented in Fig. 32. The temperature vs time curve shows the predicted inside air temperature of the east-side upper solar collector compares favorably with the measured values.

The results of the Case II study are presented in Fig. 33. The predicted air temperature curve of the east-side upper solar collector was obtained using three capacitance values for the three respective air flow values. The predicted temperature curve has the same general shape as the measured temperature curve and is very close for initial and peak values. The difference between the predicted temperature and the observed temperature resulted from using large lumped capacitors (Table 8) in the circuit simulation to account for air movement within the system. Air movement in the actual structure causes turbulence due to the geometric configuration of the structure and the boundary layer conditions. These factors will be eventually

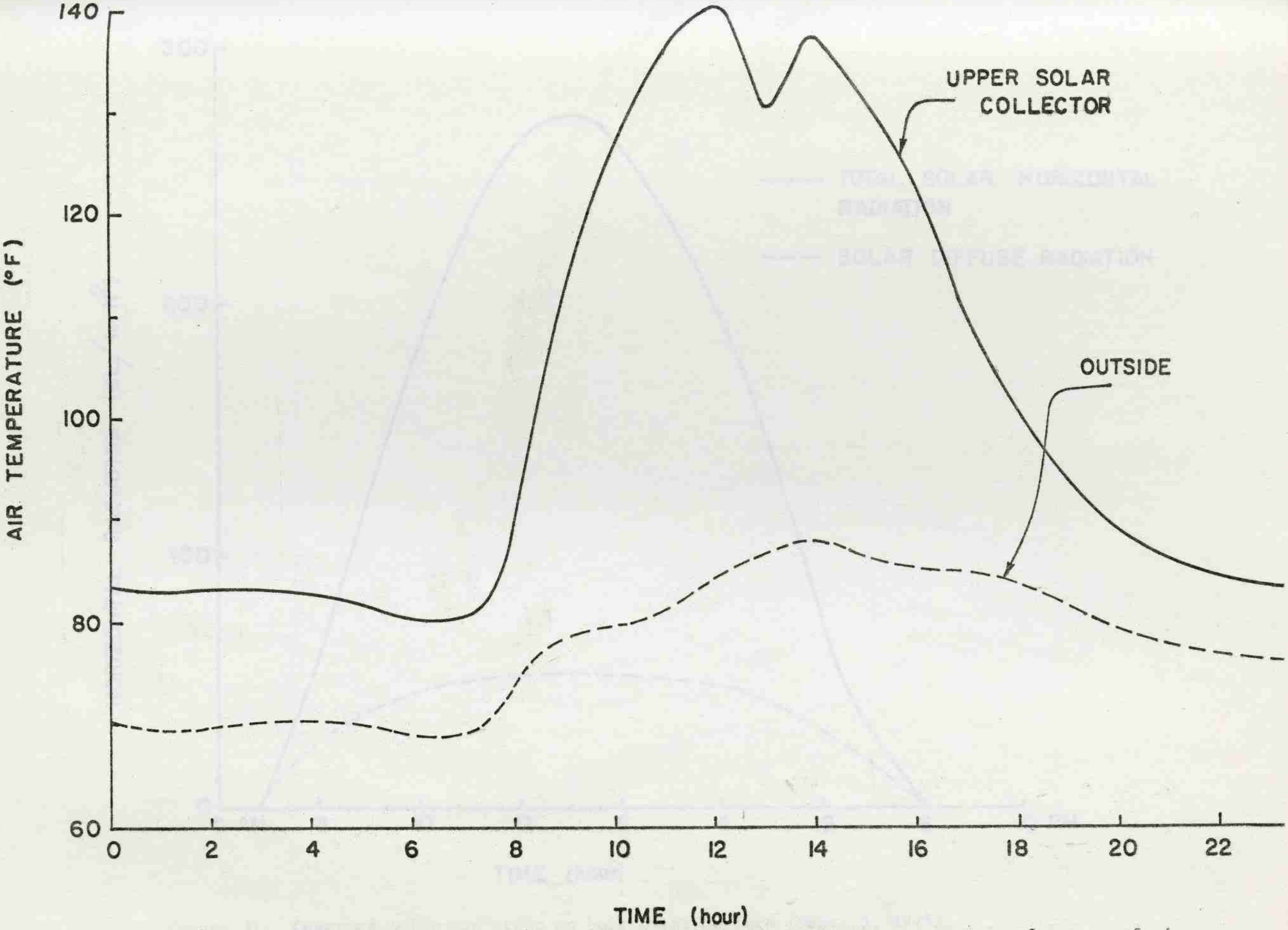

Figure 30. Diurnal variation of outside air and east-side collector air temperatures for case of air movement (Sept. 5 1975).

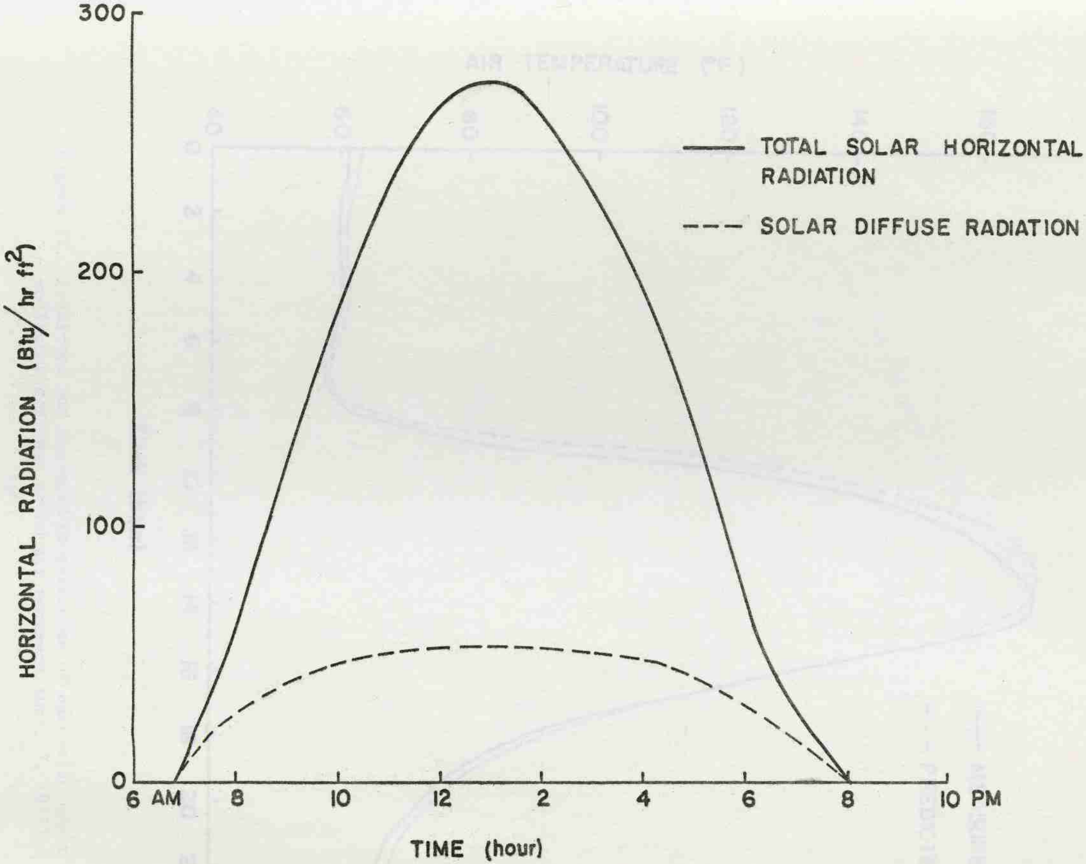

Figure 31. Observed solar radiation on horizontal surface (Sept. 5, 1975).

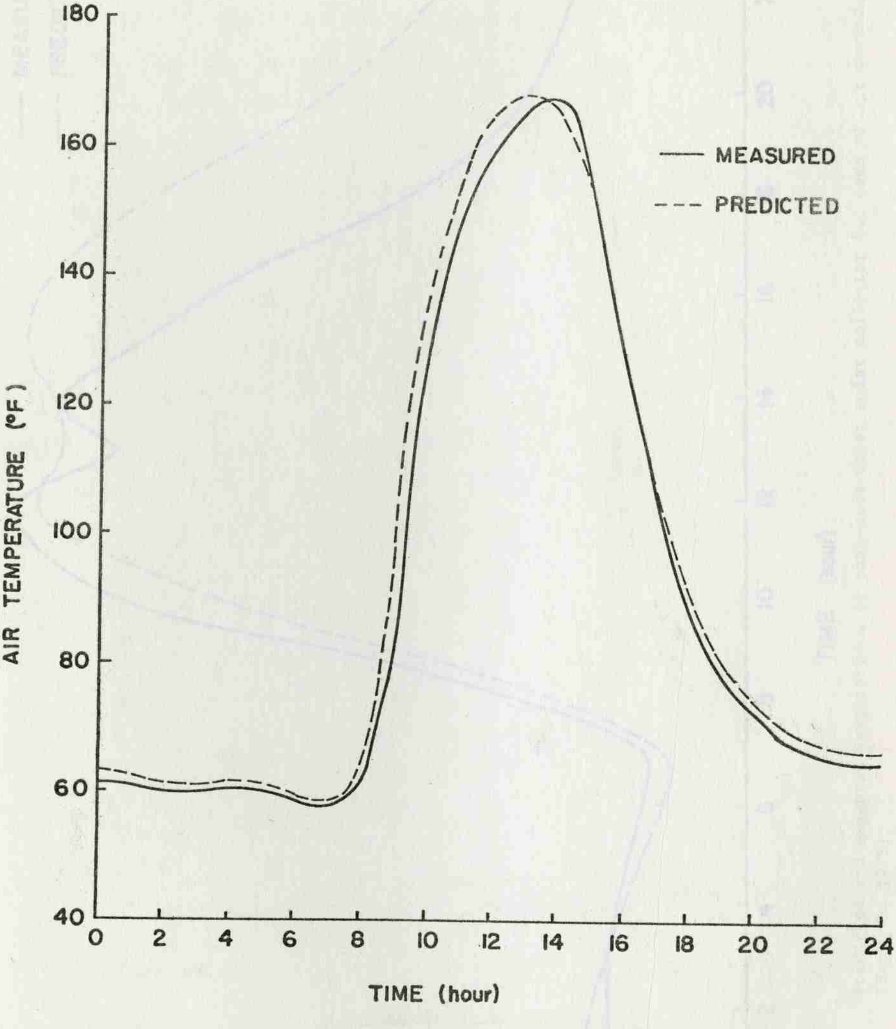

Figure 32. Predicted and measured temperatures of east-side upper solar collector for case of no air movement (Oct. 7, 1975).

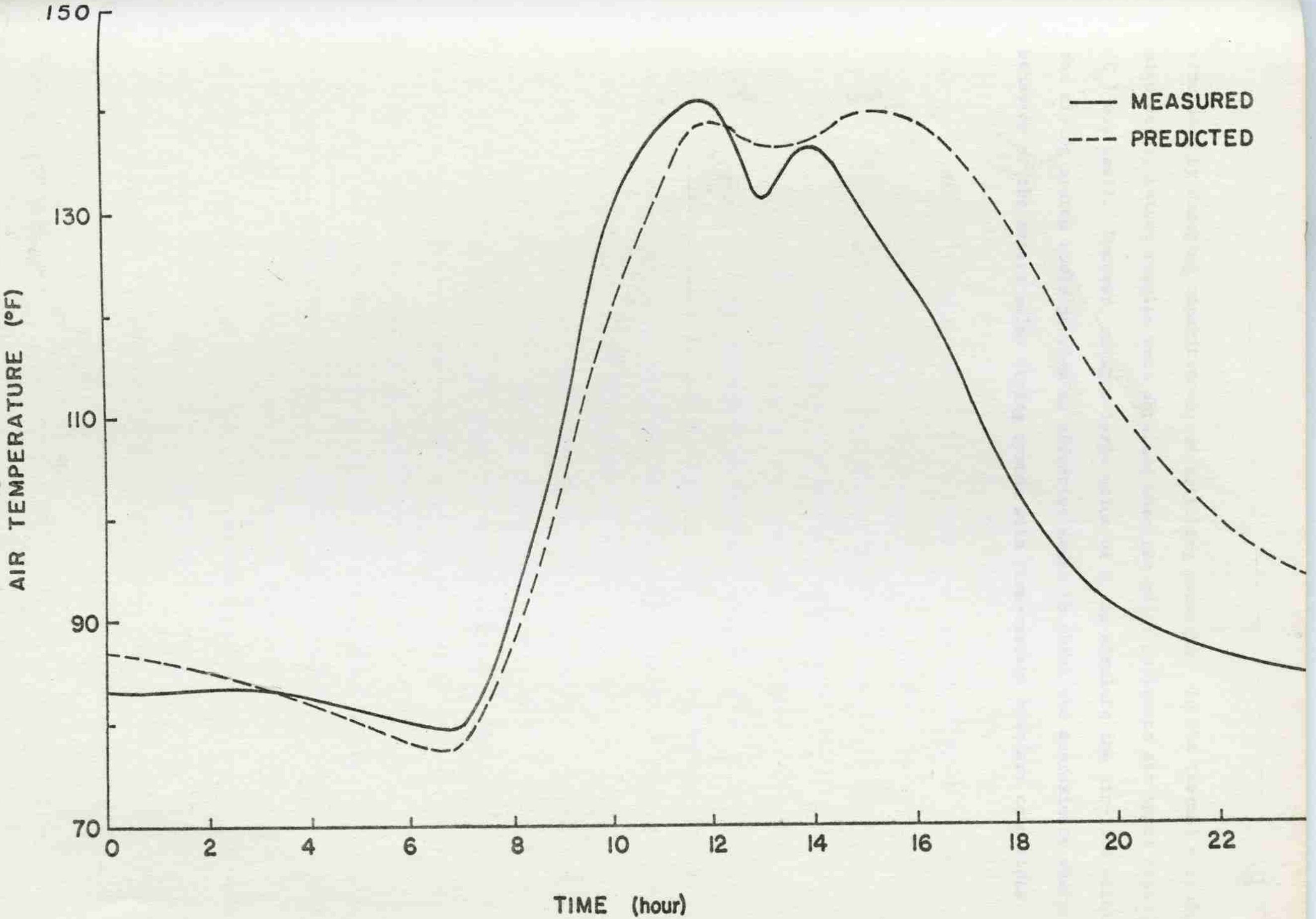

Figure 33. Predicted and measured temperatures of east-side upper solar collector for case of air movement (Sept. 5, 1975).

simulated by changing capacitances and switching networks. In the thermal circuit simulation, better results were obtained when the solar collector air space capacitor (C_a) was small. However, using a large value of C_a to simulate the air-flow within the drying system would provide an effective means to check the approximate thermal behavior of the entire solar drying system with time-variant boundary conditions.

CONCLUSIONS AND RECOMMENDATIONS

During 1975 a greenhouse bulk curing and drying system was designed, constructed and tested for solar energy utilization in the bulk curing of tobacco. The structure consists of a transparent fiberglass exterior, the black surfaced heat-absorber/insulation boards, the portable frames, and the gravel energy storage system with electric power saving features. The total structure was effectively used as an integrated solar collector during daytime for preheating air prior to being circulated through the tobacco or gravel storage system, was effectively used at night to preheat the air by using the gravel storage system, and was effectively used as an integrated heat exchanger during nighttime yellowing for dehydrating air and recovering remaining heat in the circulating air. As compared to a conventional bulk curing barn, the greenhouse bulk curing system achieved an overall fuel savings of 37 percent while maintaining good quality curing.

The system was successfully operated in the greenhouse mode to grow flowers and tobacco transplants. Equipment was easily converted from the tobacco curing mode to the greenhouse operation mode. No adverse affects of the top air duct or the black north wall were noted on the plant growth. Significant heating energy savings were also realized during greenhouse mode of operation.

A computer model is being developed to assist in further design optimization of the energy collection and storage systems. Initial results of the thermal circuit analogy for analyzing the greenhouse bulk curing and drying system predict the actual temperatures of the solar preheated air quite well. Further refinements and developments need to be made in the analysis to completely predict other temperatures and to predict the energy collection and storage features of the greenhouse bulk curing and drying system for various modes of operation for both curing and drying, and greenhouse production. Optimization of design parameters can then be readily achieved through computer simulation.

In order to increase the solar energy collection, energy storage, and space utilization the following design modifications were incorporated into the structures for improved total performance: (1) The top and side heat absorber surfaces, the top air duct and the gravel energy storage channels were extended over and by the sides of the furnace unit to the rear of the structure. The furnace room air duct shown in Figure 8 was replaced by a false floor. These changes resulted in simplified construction and easier air flow control and added approximately 28% more heat absorber area and 24% more energy storage volume as compared to the first design, (2) A middle curing chamber was added in the second design in place of the middle access pathway and gravel storage of the first design. This change increases the curing capacity of the greenhouse bulk curing and drying system without appreciably increasing the cost of the structure, (3) The gravel energy storage volume of the second structure was increased by having a wall height of 32 inches instead of 16 inches. It was determined that the air flow requirements for the auxiliary fan were much less for depth increases than for length increases. Also, increased depths of gravel are more easily accommodated in the current structure than length increases.

Any solar energy utilization device is weather dependent. In order to optimize the system functions to obtain the full utilization of incident and radiant solar energy as well as energy conservation, automatic air flow control based on temperature, humidity, available solar energy, stored solar energy, and curing requirements should be implemented. With the acquired data, computer simulations, and experience gained during the field tests under this project, the criteria for automatic control can be developed. This criteria can then be used in a microprocessor based data acquisition and control system to optimize solar energy collection, storage, and utilization and to minimize both fuel and electrical energy consumption. The electrical energy conservation should be fully tested to achieve total reduction of energy required to cure and dry flue-cured tobacco.

REFERENCES

1. ASHRAE. 1967. ASHRAE Handbook of Fundamentals. ASHRAE, Inc. New York, N.Y.

2. Bowers, C.G., B.K. Huang, and C.F. Abrams, Jr. 1975. Solar energy utilization in a bulk curing/greenhouse system. ASAE Paper No. 75-3504.

3. Hassler, F.J. 1959. Theoretical identification of a critical temperature - moisture relation in foliar drying. Trans. ASAE 2(1):48-51.

4. Holman, J.P. 1972. Heat transfer. McGraw-Hill Book Co., New York, N.Y.

5. Huang, B.K. and H.S. Chang. 1976. Circuit simulation analysis of heat transfer effect in solar drying. ASAE Paper No. 76-3019.

6. Huang, B.K. 1975. Greenhouse-bulk curing and drying system. United States Patent 3,866,334 Feb. 18, 1975. United States Patent Office, Washington, D.C.

7. Huang, B.K., C.F. Abrams, L.L. Coats, and C.G. Bowers. 1975. Development of greenhouse bulk curing system for solar energy utilization and plant-bed mechanization. ASAE Paper No. 75-1018.

8. Huang, B.K. 1974. Electronic circuit analysis program application. AGRICULTURAL ENGINEERING 55(7):52.

9. Huang, B.K. 1973. Dynamic system analogies and mathematical interpretation. ASAE Paper No. 73-5549.

10. Huang, B.K. 1972. Digital simulation analysis of biophysical systems. Trans. IEEE, BME-19(2):128-139.

11. Johnson, W.H. 1963. The bulk curing process for bright-leaf tobacco. ASAE Paper No. 63-125.

12. Kent's Mechanical Engineer's Handbook. 1923.

13. Knox, R.E. Insulation properties of fluorocarbon expanded rigid urethane foam. Trans. ASHRAE, Vol. 69, p. 150.

14. Ozisik, M.N. 1973. Radiative transfer and interactions with conduction and convection. John Wiley and Sons, Inc., New York, N.Y.

APPENDIX A

GREENHOUSE BULK CURING AND DRYING SYSTEM CONSTRUCTION

GREENHOUSE BULK CURING AND DRYING SYSTEM CONSTRUCTION

The greenhouse bulk curing structure foundation, Figure 34, consists of a 4 inch concrete slab, 27 feet wide by 46 feet long, with 6 inch concrete footings, concrete reinforcing wire, and a 4 mil polyethylene plastic vapor barrier. Two courses of 8 inch by 8 inch by 16 inch concrete blocks form the foundation walls for the upright structure and the portable frame tracks on each side of the air plenum. Eight inch corrugated and perforated plastic pipes are covered by approximately 20 tons of crushed granite to form gravel storage areas on the sides and middle of the foundation.

The upright structure is an X.S. Smith, Inc. Criterion Greenhouse, 25 feet wide by 44 feet long by 12 feet high. (The advantage of adaptability of a commercially available structure may encourage acceptance of the greenhouse bulk curing system). Aluminum pipe (1 1/4 inch) spaced every 4 feet form the supporting bows for the corrugated, Tedlar coated fiberglass. End framing was not supplied by the greenhouse manufacturer and was made with 2 inch square tubing and 1 1/4 inch galvanized pipe as shown in Figures 6 and 7. Doors on the front and back of structure are made with 1 1/2 inch square steel tubing. All framing members are painted black for increased solar energy collection. Doors and ends are covered with flat fiberglass.

Interior walls separate the curing/growth chamber, furnace room and instrument room. These walls consist of 2 inch by 4 inch treated wood framing and 1/2 inch exterior plywood. Return openings are cut for the furnace and air duct.

The heating unit is a standard furnace used in mobile bulk barns manufactured by Harrington Manufacturing Company. It is an LP unit rated at 840,000 BTU/hour with a 15,000 cubic feet/minute air flow provided by an axial flow fan. Automatic temperature control from $40^{o}F$ to $200^{o}F$ with automatic temperature advance are

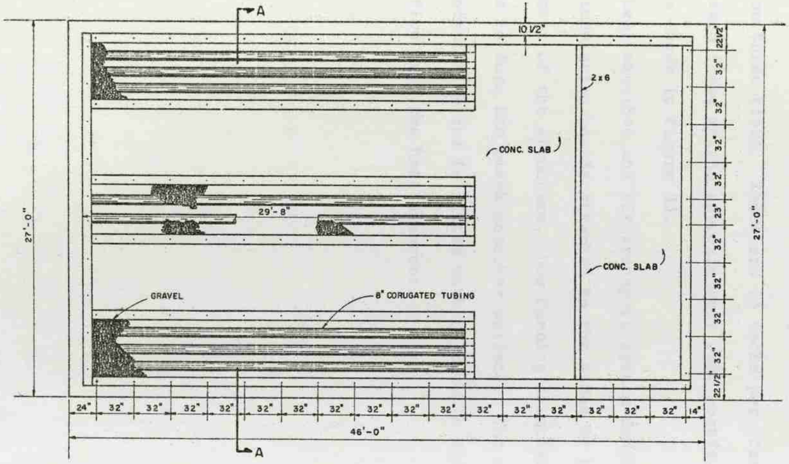

FOUNDATION PLAN
SCALE- 1/4" = 1'-0"

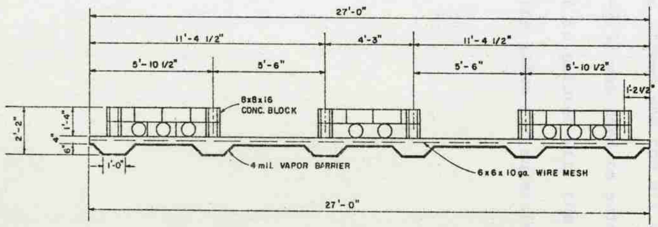

SECTION A-A
SCALE- 3/8" = 1'-0"

Figure 34. Foundation of greenhouse bulk curing and drying system.

provided on the unit. An air mixing chamber is constructed at the bottom of the furnace as shown in Figure 8.

The portable frames with one side covered with 1/4 inch exterior plywood were made of two inch square tubing and 2 inch angle iron. Conventional bulk curing racks slide in on three tiers. There are 15 racks per frame; and when filled with green tobacco, each frame weighs approximately 3000 pounds. Details of the portable frame design are shown in Figure 35.

The heat absorber and air transport system consist of light aluminum faced polyurethane insulation boards attached to the sides of portable frames and the air duct in the center of the structure. Dow Corning formulation E1-9752 was used to paint the boards to form the black absorber surface. The air duct is painted with the Dow Corning formulation and is fitted with adjustable doors on the sides for maintaining even air flow over the heat absorber.

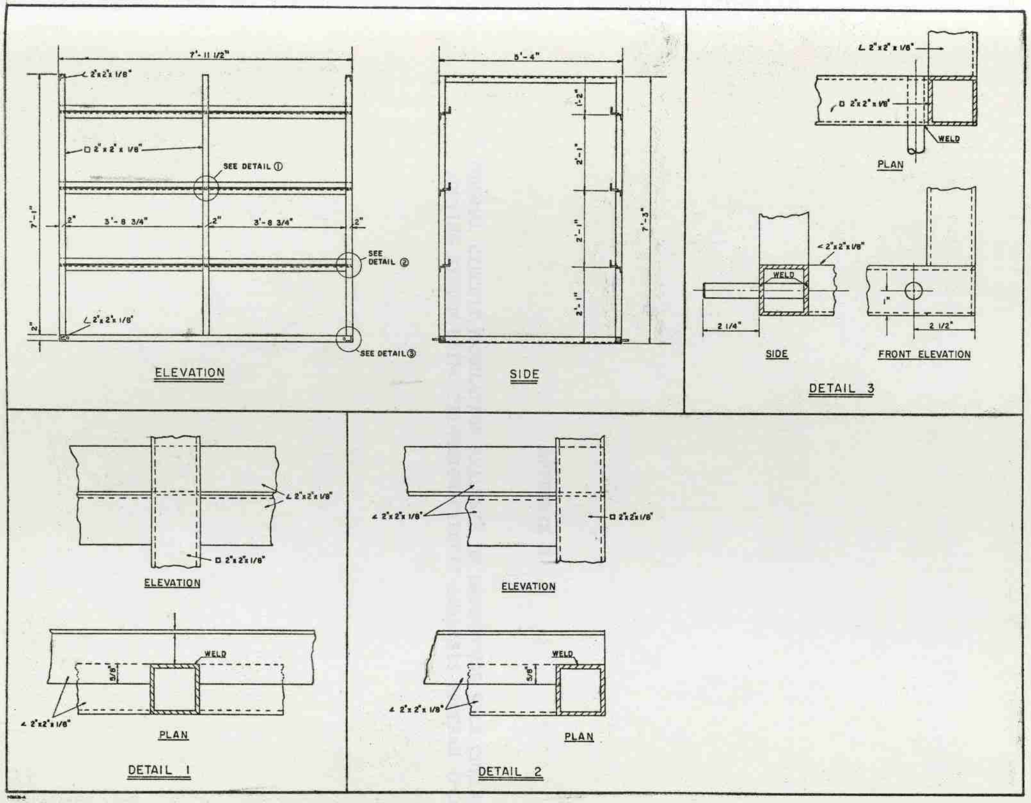

Figure 35. Portable frame used in greenhouse bulk curing and drying system.

APPENDIX B

THERMAL CIRCUIT SIMULATION ANALYSIS OF GREENHOUSE BULK CURING AND DRYING SYSTEM USING PRINCETON CIRCUIT ANALYSIS PROGRAM (PCAP)

TRANSIENT ANALYSIS

```
C
B1     N(1,0),R=41.2E3
E1     P(0.5),
      *70.1,68.5,68.0,69.0,69.8,69.0,67.6,68.0,73.0,77.6,79.5,81.0,
      *83.6,86.0,88.0,86.5,87.0,86.0,84.0,81.0,79.0,78.0,76.5,75.0,70.1
B2     N(1,2),R=5.0E3
B3     N(2,0),C=2.10E-6
B4     N(2,3),R=5.0E3
B5     N(24,3),R=144.2E3
B6     N(4,0),R=0.001E3
E6     P(0.5),
      *70.1,68.5,68.0,69.0,69.8,69.0,67.6,68.0,73.0,77.6,79.5,81.0,
      *83.6,86.0,88.0,86.5,87.0,86.0,84.0,81.0,79.0,78.0,76.5,75.0,70.1
B7     N(4,5),R=646.4E3
B8     N(5,6),R=78.7E3
B9     N(6,0),C=0.13E-6
B10    N(6,7),R=78.7E3
B11    N(24,7),R=1801.1E3
B12    N(8,24),R=99.4E3
I12    P(0.5),
      *0.0,0.0,0.0,0.0,0.0,0.0,0.0,-0.18E-3,-0.68E-3,-1.37E-3,-1.92E-3,
      *-2.35E-3,-2.56E-3,-2.59E-3,-2.17E-3,-1.66E-3,-1.12E-3,-0.55E-3,
      *-0.20E-3,-0.04E-3,0.0,0.0,0.0,0.0,0.0
B13    N(8,9),R=0.00005E3
B14    N(9,0),C=0.16E-6
B15    N(9,10),R=144.8E3
B16    N(10,0),C=0.84E-6
B17    N(10,11),R=144.8E3
B18    N(11,0),C=0.16E-6
B19    N(11,12),R=0.00005E3
B20    N(12,0),R=5000.0E3
E20    P(0.5),
      *70.1,68.5,68.0,69.0,69.8,69.0,67.6,68.0,73.0,77.6,79.5,81.0,
      *83.6,86.0,88.0,86.5,87.0,86.0,84.0,81.0,79.0,78.0,76.5,75.0,70.1
B21    N(13,24),R=430.1E3
I21    P(0.5),
      *0.0,0.0,0.0,0.0,0.0,0.0,0.0,-0.20E-3,-0.34E-3,-0.50E-3,-0.51E-3,
      *-0.43E-3,-0.26E-3,-0.085E-3,-0.085E-3,-0.082E-3,-0.082E-3,
      *-0.075E-3,-0.062E-3,-0.034E-3,0.0,0.0,0.0,0.0,0.0
B22    N(13,14),R=0.02E3
B23    N(14,0),C=2.61E-6
B24    N(14,15),R=0.02E3
B25    N(15,0),R=5000.0E3
E25    P(0.5),
      *70.1,68.5,68.0,69.0,69.8,69.0,67.6,68.0,73.0,77.6,79.5,81.0,
      *83.6,86.0,88.0,86.5,87.0,86.0,84.0,81.0,79.0,78.0,76.5,75.0,70.1
B26    N(16,24),R=1801.1E3
I26    P(0.5),
      *0.0,0.0,0.0,0.0,0.0,0.0,0.0,0.0,-0.02E-3,-0.05E-3,-0.08E-3,
      *-0.10E-3,-0.12E-3,-0.13E-3,-0.11E-3,-0.10E-3,-0.08E-3,-0.06E-3,
      *-0.03E-3,-0.02E-3,0.0,0.0,0.0,0.0,0.0
B27    N(16,17),R=290.1E3
B28    N(17,0),C=1.57E-6
B29    N(17,18),R=290.1E3
B30    N(18,0),R=5000.0E3
B31    N(23,19),R=1187.1E3
B32    N(19,22),R=1135.1E3
B33    N(21,19),R=230.1E3
B34    N(19,20),R=70.1E3
B35    N(21,20),R=445.1E3
B36    N(23,21),R=5478.6E3
B37    N(22,21),R=5635.5E3
B38    N(20,22),R=2735.6E3
B39    N(23,22),R=71221.7E3
B40    N(20,23),R=2739.3E3
B41    N(3,19),R=2.4E3
B42    N(7,23),R=37.5E3
B43    N(16,22),R=37.5E3
B44    N(13,21),R=8.9E3
B45    N(8,20),R=2.9E3
B46    N(24,0),C=44.1E-6
E46    P(0.5),
      *83.5,80.7,78.5,77.4,76.3,74.6,73.6,78.0,92.5,105.0,112.5,116.5,
      *120.6,117.5,113.5,111.0,108.0,105.0,101.0,97.5,94.5,92.0,
      *88.0,87.0,83.5
       TI=0.1
       OU=5
       FI=36.0
       PLOT,NV(24)
       EX
```

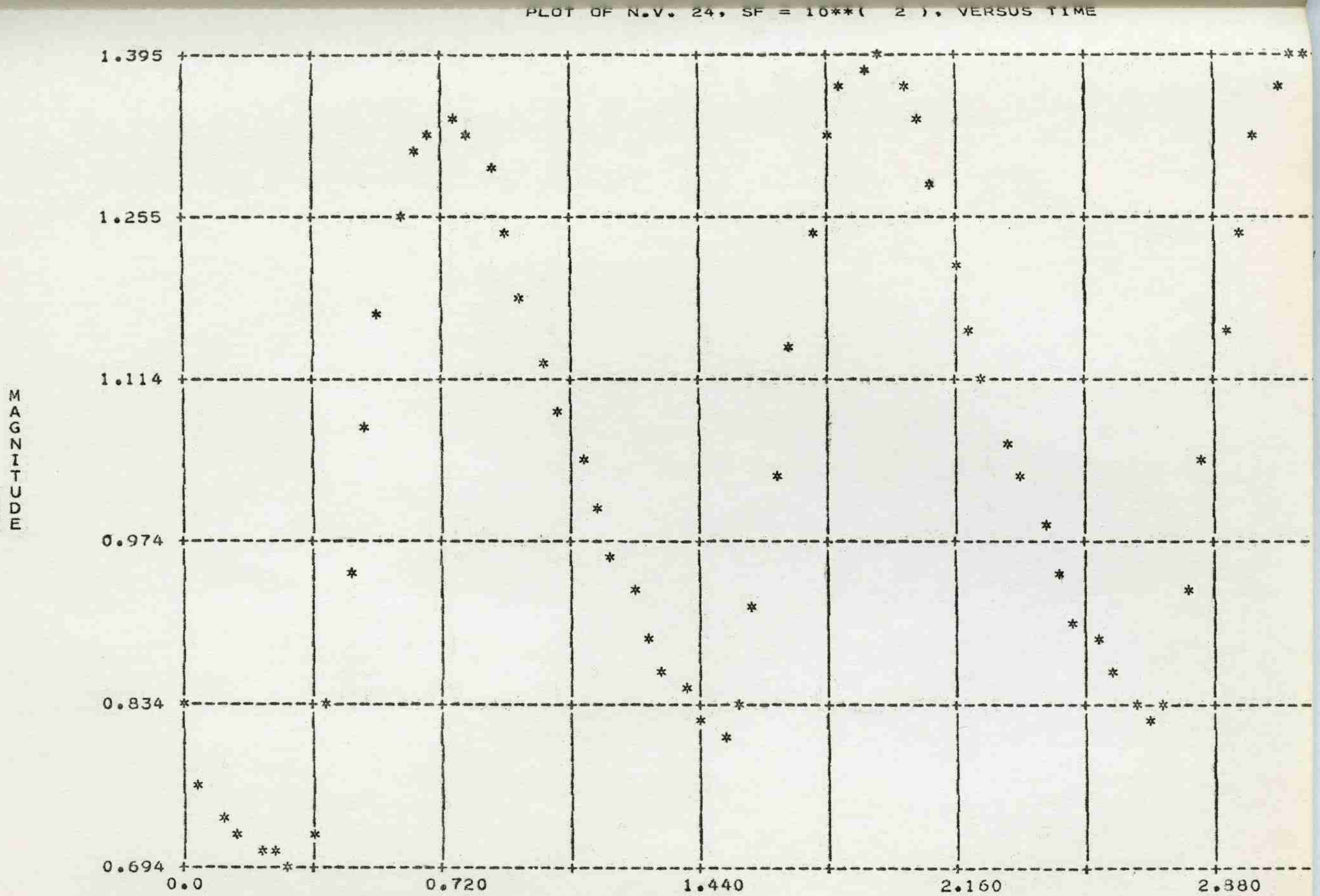

Figure 36. Computer plot of thermal circuit simulation results.